The Role of Carbonate Bedrock in the Formation of Indianaite Halloysitic Clays

INDIANA UNIVERSITY INDIANA GEOLOGICAL SURVEY

Bulletin 65

STAFF OF THE INDIANA GEOLOGICAL SURVEY

ADMINISTRATION (Phone 812/855-5067)
Norman C. Hester, Director/State Geologist
John R. Hill, Assistant Director
Pat Gerth, Secretary (Director and Asst. Dir.)
Charlotte Smith, Financial Officer
Helen Stephenson, Financial Records Assistant
Tammy Watson, Certification Secretary

BASIN RESEARCH COORDINATOR (Phone 812/855-4213)
Brian Keith, Petroleum Geologist

EDUCATION EXTENSION (Phone 812/855-7636)
John R. Hill, Geologist and Head
Jeff Kirby, Assistant Geologist

ENERGY RESOURCES SECTION (Phone 812/855-5412)
John A. Rupp, Geologist and Head
Jerry R. Burton, Geologic Technician
James T. Cazee, Cartographic Specialist and Geologic Draftsman
Sherry Cazee, Sample and Core Library Supervisor
Lloyd Furer, Stratigrapher
Stanley J. Keller, Petroleum Geologist
Maria Mastalerz, Coal Geologist
Todd Thompson, Sedimentologist
Charles W. Zuppann, Petroleum Geologist

ENVIRONMENTAL SECTION (Phone 812/855-7428)
Edwin J. Hartke, Geologist and Head
N. K. Bleuer, Glacial Geologist
Steve Brown, Glacial Geologist
Donald L. Eggert, Environmental Geologist
Anthony Fleming, Glacial Geologist
John Haddan, Field Laboratory Technician
Denver Harper, Environmental Geologist
Nancy Hasenmueller, Environmental Geologist
Ray René, Geophysicist
Carl B. Rexroad, Paleontologist
M. Sue Shaver, Secretary

GEOCHEMISTRY (Phone 812/855-2687)
John B. Comer, Head
Tracy Branam, Geochemist
Marilyn DeWees, Secretary
Margaret V. Ennis, Geochemist

INDUSTRIAL MINERALS PRINCIPAL GEOLOGIST (Phone 812/855-2687)
Donald D. Carr, Geologist

MINERAL RESOURCES (Phone 812/855-2687)
Henry L. Barwood, Head
Marilyn DeWees, Secretary
Walter A. Hasenmueller, Geologist
Kathryn R. Shaffer, Mineral Statistician
Nelson R. Shaffer, Geologist

PHOTOGRAPHY SECTION (Phone 812/855-1370)
Barbara T. Hill, Head
John Day, Photographic Specialist

PHYSICAL FACILITIES AND FIELD SERVICES (Phone 812/855-3596)
Sam Frushour, Head
Jay Arnold, Drilling Foreman
Thomas Chitwood, Geologic Technician
Sam Riddle, Driller

PROGRAM COORDINATOR (Phone 812/855-1351)
Gordon S. Fraser, Geologist

TECHNOLOGY TRANSFER SECTION (812/855-7636)
Richard T. Hill, Head

EDITORIAL (Phone 812/855-7636)
Deborah DeChurch, Editor

GRAPHICS AND CARTOGRAPHY (812/855-5893)
Rea Kersey, Cartographic Specialist
Kari Lancaster, Cartographic Specialist
Roger Purcell, Senior Cartographic Specialist
Kimberly Sowder, Senior Cartographic Specialist
Wilbur Stalions, Cartographic Specialist

INFORMATION TECHNOLOGY (Phone 812/855-7636)
Paul Irwin, GIS/Database Analyst

PUBLICATION SALES (Phone 812/855-7636)
Janis Fox, Senior Publications Assistant
Pat Gerth, Publications Specialist/Associate Head

For sale by Publication Sales, Indiana Geological Survey,
611 N. Walnut Grove, Bloomington, Indiana 47405

The Role of Carbonate Bedrock in the Formation of Indianaite Halloysitic Clays

By Clifford P. Ambers *and* Haydn H. Murray

INDIANA UNIVERSITY
INDIANA GEOLOGICAL SURVEY BULLETIN 65

BLOOMINGTON, INDIANA: 1995

AUTHORS

Clifford Ambers is a visiting research scientist at the University of Oklahoma School of Geology and Geophysics.
Haydn Murray is an emeritus professor and retired chairperson of the
Indiana University Department of Geological Sciences.

CONTENTS

ILLUSTRATIONS

THIS PAGE INTENTIONALLY LEFT BLANK

THE ROLE OF CARBONATE BEDROCK IN THE FORMATION OF INDIANAITE HALLOYSITIC CLAYS

By Clifford P. Ambers *and* Haydn H. Murray

ABSTRACT

Indianaite is a rock term for halloysite- (10Å) and allophane-rich clays that generally occur as layered, bedding-parallel bodies in the shallow subsurface of south central Indiana. These clays have received considerable attention from geologists because of their enigmatic genesis and by industry because of their value as raw material for ceramics, catalysts, and alum manufacture. Recent exposures of indianaite deposits in limestone quarries near Bloomington and Bedford, Indiana, reveal aspects of indianaite structure, texture, and stratigraphic placement that clearly indicate its origin. These deposits were examined in the field and in the laboratory by scanning electron microscopy, x-ray diffraction, differential thermal/ thermal gravimetric analysis, and optical petrography to document features indicating genetic mechanisms. Results of these analyses were combined with published data from the previously mined deposit at Gardner Mine Ridge near Huron, Indiana, to develop a model for the genesis of indianaite. Mineral-water reactions hypothesized to have operated in the formation of indianaite are supported by field and laboratory observations.

Results of this study indicate that indianaite forms by the interaction of aluminosilicate detritus with vadose water acidified by iron-sulfide oxidation followed by neutralization of this ion-charged fluid by contact with limestone which causes precipitation of indianaite minerals. Replacement of iron sulfides by limonite, replacement of limestone by gypsum, and precipitation of hydrous aluminous phases adjacent to the limestone/gypsum are the major indicators of this process. Mineral transformations occur in the aluminous precipitates with time and changes in pH. Increases in pH occur as fluids equilibrate with the carbonate substrate, and lowering of pH may be caused by changes in fluid migration pathways through the precipitate. Formation of indianaite requires that a superadjacent siliciclastic unit rich in iron sulfide be exposed at the weathering surface and that the subadjacent carbonate unit lies at least partially above the water table. This prerequisite juxtaposition of rock types sets the stage for: 1) oxygenated rain waters to react with iron sulfides to produce sulfuric acid; 2) interaction of the acid with aluminosilicates in the siliciclastic unit; 3) migration of the fluid downward to the limestone; and 4) precipitation of aluminous minerals as the pH rises above 4 in the fluid as it contacts the limestone. Precipitation of indianaite along cave walls suggests that continued downward migration of vadose waters rather than lateral flow at the limestone interface causes dispersed mineralization down subterranean drainages preventing formation of a thick, layered deposit. Thick deposits like the Gardner Mine Ridge deposit are hypothesized to have formed where the fluid migration became horizontal allowing the complete dissolution of the limestone and replacement by indianaite.

Precipitation of aluminous indianaite minerals by the interaction of aluminum-charged, acidified water with limestone extends to other published examples of halloysitic clays which form adjacent to and as replacements of limestone or dolostone. Future exploration for indianaite will benefit from the constraints on indianaite genesis presented here. Study of available logs and cores should provide enough information to delimit potential resource areas and confirmatory drilling and field work could easily prove or refute a suspected deposit.

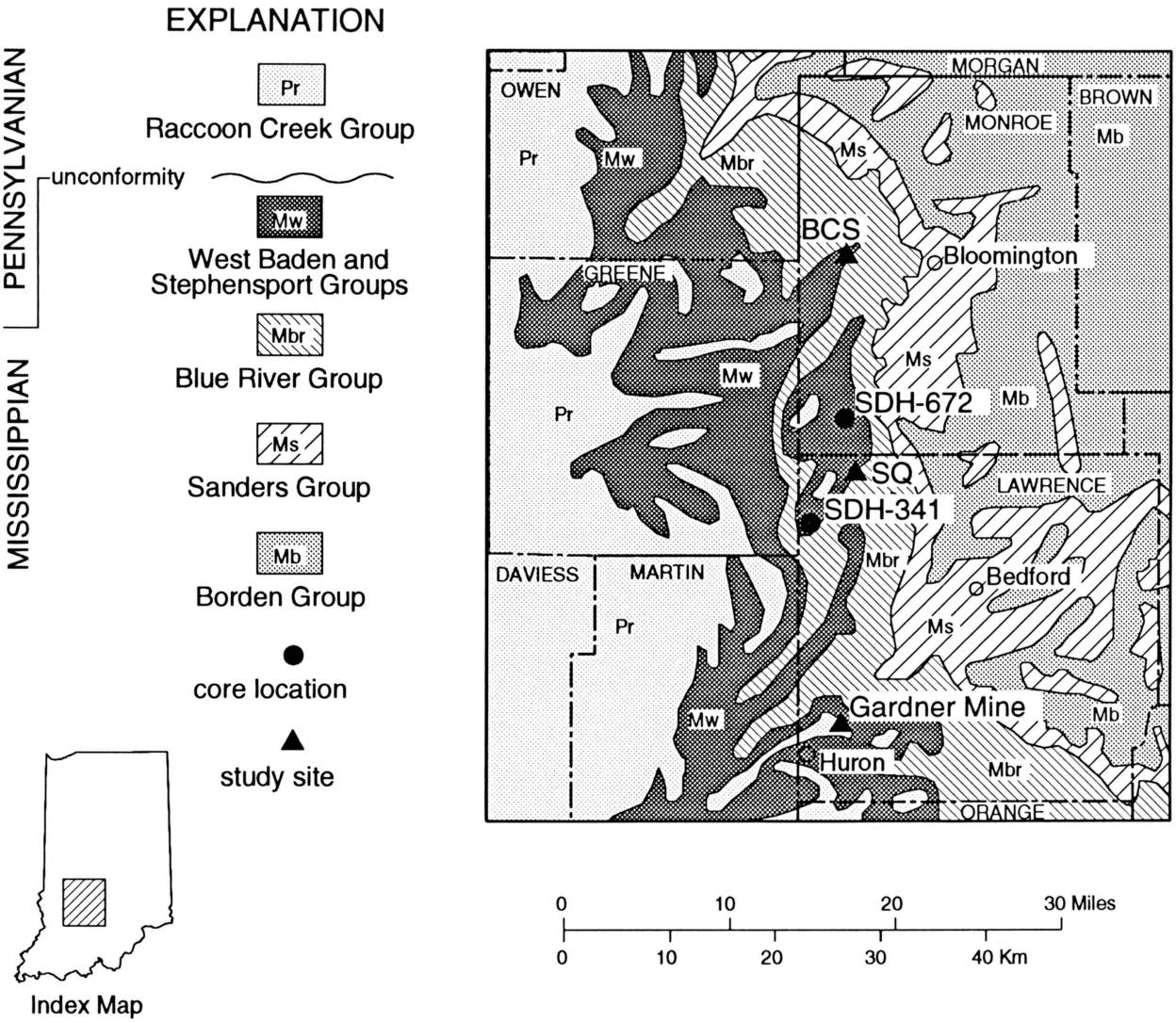

Figure 1. Generalized geologic map showing locations of indianaite deposits discussed in text. (After Gray, 1990.)

INTRODUCTION

Exposure of indianaite in 1991 during excavation at the Bloomington Crushed Stone Company (BCS) quarry near Bloomington, Indiana (fig. 1) prompted this study. Indianaite is a field term proposed by Cox (1875, 1879) for white, green, or purplish brown mudrock containing halloysite ± allophane ± kaolinite ± gibbsite ± quartz ± Al, Ca, Fe sulfates ± Fe, Mn oxyhydroxides ± Al, Ca phosphates. Indianaite is not a monomineralic rock made of halloysite (as discussed by Shaffer, 1978), therefore the rock term "halloysite" is not used here for these materials. Data from BCS were used to predict the occurrence of indianaite at the Sieboldt Quarry (SQ) near Bedford, Indiana. New data from BCS and SQ was compared with existing information from the well-known deposit at Gardner Mine Ridge (GMR) near Huron, Indiana, to formulate a genetic model for the indianaite at the three localities (fig. 1).

The mechanism of indianaite precipitation has been discussed since its initial description by Cox (1875). Nearly all of the models agree that sulfuric acid waters derived from FeS weathering have altered alumina- and silica-bearing minerals to produce an aluminous deposit (Cox, 1875; Thompson, 1886; Logan, 1922a, b; Ries, 1922; Callaghan, 1948; Kildale and Thomas, 1957; Greenberg and Sunderman, 1961; Crawford and McGrain, 1963; Sunderman, 1963; Keller and others, 1966; Huang and Keller, 1973; Dombrowski and others, 1988; Ettensohn and Bayan, 1990). Early publications tended to favor alteration of a precursor clay unit to produce indianaite *in situ*, whereas more recent studies suggest a combination of precursor clay alteration and dissolution of aluminosilicates in acid water and precipitation of indianaite. In both old and new studies, however, the mechanisms of indianaite mineral precipitation or alteration of precursor clay to indianaite minerals are not well defined nor are they supported by textural evidence or spatial relationships of adjacent rock bodies.

Exposures at BCS and SQ provide strong textural evidence for the mechanism of indianaite emplacement. Conclusions of this study for the BCS and SQ deposits are based on field observations and X-ray diffraction, thermal analysis, scanning electron microscopy, and optical petrography. Comparison of our results to published information from the GMR deposit shows conclusively that indianaite formation is the result of *direct* interaction of sulfuric acid waters with limestone. This model extends to other examples of sulfate-generated halloysitic clay deposits.

Indianaite was once exploited for ceramic and chemical uses (Shaffer, 1978) and interest in these unique clays continues. GMR was the center of indianaite production from the late 1800s through the 1920s. Much of the material removed was shipped to Philadelphia for alum manufacture primarily for water softening purposes. This study serves as a basis for further exploration for indianaite.

METHODS

Field observations included documentation of rock types, thicknesses, colors (Rock-Color Chart Committee, 1984), and relative positions of adjacent rock bodies and mineral aggregates. Samples were taken sequentially through the mineralized zones at BCS and SQ, which were subdivided vertically into zones of unique texture and color. To assess mineralogy, samples were ground in an agate mortar and pestle with distilled water and scanned wet from 2 to 60 degrees 2θ on a Scintag automated X-ray diffraction (XRD) unit using Cu-Kα radiation, a Ni monochromator and an accelerating voltage of 45 KV. Detailed clay identification was performed on <2μm oriented samples scanned from 2 to 60 degrees 2θ in air dried, glycolated, heated to 325°C, and heated to 500°C states. Mounts of each sample were coated with Au-Pd and viewed on a Cambridge Stereoscan model 250 MK2 scanning electron microscope (SEM) equipped with a Tracor Northern energy dispersive X-ray detection system and a standard tungsten filament. Rocks immediately below the indianaite were examined petrographically. Differential thermal and thermal gravimetric analyses (DTA/TGA) of indianaite were made using a heating rate of 10°C per minute and alumina as a reference standard (Mackenzie, 1970). Samples for DTA/TGA were equilibrated in a closed cell with 76 percent relative humidity provided by a saturated solution of oxalic acid containing excess solute at 20°C.

GEOLOGIC SETTING

Locations of 46 indianaite occurrences in Indiana are given in Logan (1922b). The map pattern forms a 20-mile-wide belt extending northward 80 miles from Crawford County to northern Monroe County (fig. 1). This area is underlain by upper Mississippian rocks with a few ridge tops capped by lower Pennsylvanian sandstones and conglomerates (fig. 2). A pronounced unconformity exists between Mississippian and Pennsylvanian rocks in Indiana (Droste and Keller, 1989). Basal Pennsylvanian strata commonly overlie resistant upper Mississippian limestone units in the study area (Droste and Keller, 1989, p. 8). Indianaite occurs in the Blue River Group (limestone with minor shale and dolostone), the West Baden and Stephensport Groups (interlayered siliciclastic and limestone units), and the Raccoon Creek Group (dominantly massive sandstone in the vicinity of the outcrops studied). Siliciclastic beds of the lower West Baden Group and most of the Raccoon Creek Group sediments commonly are organic-rich and pyritic where fresh. The BCS and SQ deposits occur at the boundary of the Paoli Limestone and Bethel Formation (Blue River and West Baden Groups). The GMR deposit occurs at the boundary of the Beech Creek Limestone and Mansfield Formation (Stephensport and Raccoon Creek Groups). Indianaite deposits have not been described at these horizons deeper in the subsurface to the west. Cores available at the Indiana Geological Survey do not contain indianaite at these horizons.

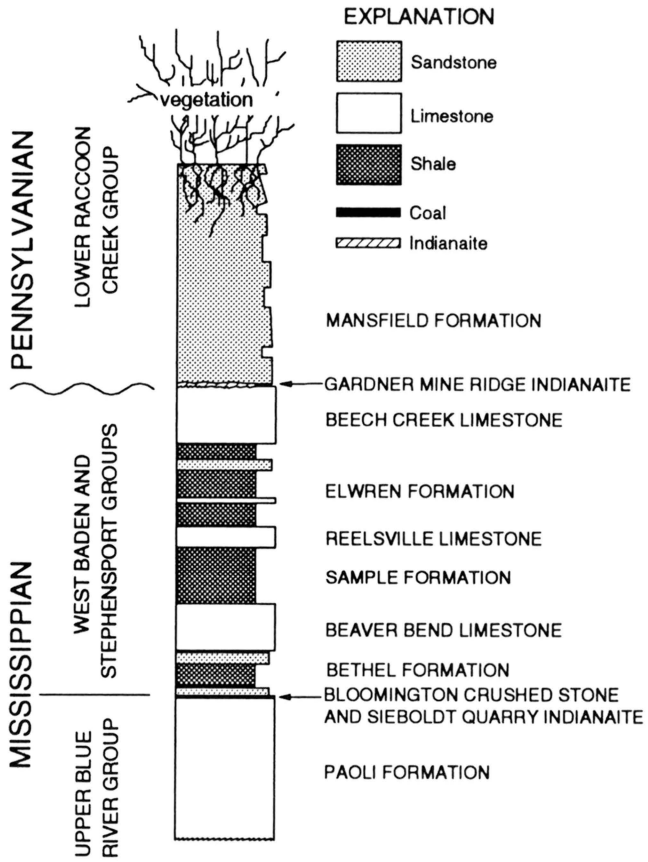

Figure 2. Stratigraphic column for the rocks studied. Positions of the indianaite deposits discussed in the text are indicated. (After Shaver and others, 1986.)

RESULTS

Field Observations

Bloomington Crushed Stone Company quarry is located in the SW¼ NE¼ section 34, T. 9 N., R. 2 W., Monroe County, Indiana. Quarrying operations are in the Blue River Group limestones and require removal of the lower West Baden Group shales and limestones. The quarry was expanded in early 1991 by removal of 2-6 m of Bethel Formation (fig. 2) from an approximately 1000 m^2 area (fig. 3A). At BCS, the Bethel consists of yellow (5Y7/2) and gray (N5) shales and 0-30 cm of clayey, medium-grained quartz sandstone at the base. Yellow shale, which contains abundant woody plant roots, extends for 2 m below the soil surface. As much as 4 m of gray shale occurs between the yellow shale and the basal sandstone (fig. 3A). The contact between the yellow and gray shales is gradational over 30 cm, and shale of both colors is moderately plastic. Vertical joints 10-30 cm apart give the gray shale a blocky appearance. Joint surfaces are coated with yellow clay (5Y7/6) and yellow staining extends from the joints into the gray clay as far as 1 cm. Woody roots (modern tree roots) are common in the joints. The basal sandstone contains abundant ripple marks, burrows, sole marks, and, where the sandstone is not limonite-stained, fragments of fusain as large as 2 cm across. Basal sandstone is missing only over a small portion of the stripped surface where it was not deposited on substrate highs (fig. 3B). The surface between the base of the sandstone and the top of the Paoli Limestone has as much as 20 cm relief. The upper Paoli Formation is a dense, medium to coarse, oolite skeletal grainstone with minor quartz sand. A silicified limestone layer as much as 6 cm thick is common at the top of the Paoli Formation but is patchy in its development. Between the limestone and the basal Bethel Formation sandstone is a discrete, white (5B9/1), porcelaneous clay layer 0.1-10 cm thick enclosed in soft, brown (10YR6/6 to 5YR3/2) iron and manganese oxyhydroxides (fig. 3C). Porcelaneous clay commonly contains black pyrolusite fracture coatings. Where the silicified limestone is missing at the top of the Paoli Formation, the oxyhydroxide layer is underlain by friable limestone containing abundant Fe-Mn oxyhydroxides. Where the silicified limestone is present, the chert is incorporated into the mineralized zone with little disruption (commonly enclosed in Fe-Mn oxyhydroxides below the porcelaneous clay layer) with the friable limestone at some position below the chert. Fractures in the limestone below the friable layer commonly contain dendritic pyrolusite which radiates upward to the friable layer where the pyrolusite is disseminated. Small caves (enlarged joints) in the Paoli Limestone below the basal sandstone of the Bethel Formation are exposed at several places. Parent joints of the caves extend through the overlying sandstone and probably did extend through

3A. Cross section of the Bethel Formation "B" and upper surface of the Paoli Formation limestone "P" in the area stripped during January 1991. The stripped surface is coincident with the indianaite layer. Cut bank is approximately 6 m high.

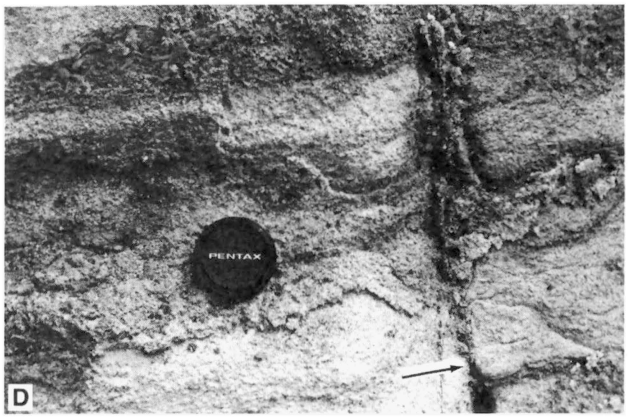

3D. Gibbsite crust coating the exposed surface of a cave in the upper Paoli Formation exposed during quarrying operations. Note the encrustation and enlargement of the vertical joint (arrow).

the shale. Caves are of two types: open caves with indianaite surface coatings (fig. 3D) and caves filled with banded indianaite and sand/yellow clay washed into the cave from the Bethel Formation along the original joint (fig. 3E). Banding in the fill parallels the cave walls. Recent woody plant roots are common in the filled caves.

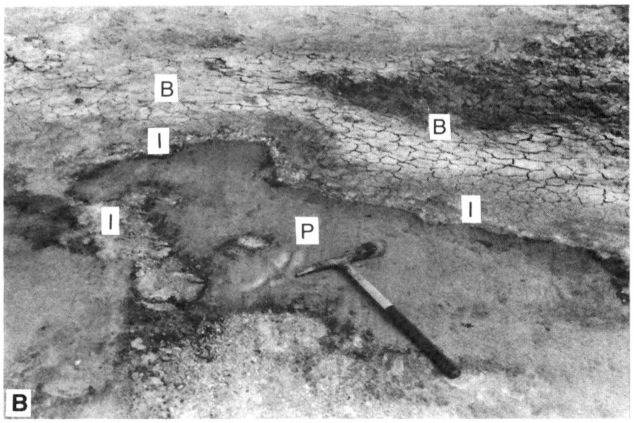

3B. View of the stripped surface with mud-cracked lower Bethel Formation sandy shale "B" surrounding friable upper Paoli Formation limestone "P." White and black indianaite "I" mineralization between the claystone and friable limestone is exposed because the mildly undulose surface separating the Bethel and Paoli Formations was intersected by the plane of stripping.

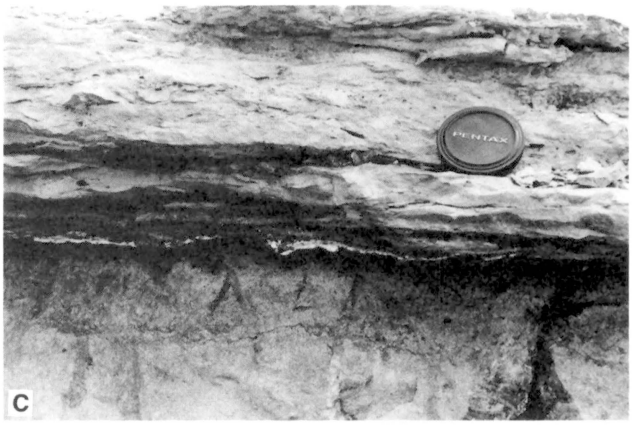

3C. View normal to bedding at the zone of indianaite mineralization separating Basal Bethel Formation sandstone above from friable upper Paoli Formation limestone below. 10 mm of black, Fe-Mn oxyhydroxide-stained, friable limestone occurs directly below 5-10 mm of white indianaite.

3E. Enlarged joint in the upper Paoli Formation limestone filled with banded indianaite and washed in sand and clay. Overlying clayey sandstone of the Bethel Formation was excavated to expose the cave fill. Note U.S. quarter (2.43 cm in diameter) for scale (arrow).

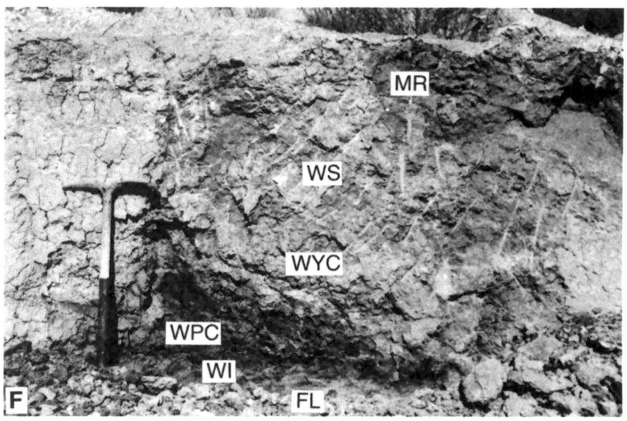

3F. Materials overlying indianaite at SQ: MR = mottled red/gray clay, WS = weathered sandstone, WPC = waxy pyrolusitic clay, WYC = waxy yellow gypsiferous clay, WI = white indianaite, FL = friable limestone.

Figure 3. Photographs showing relationships of indianaite to host rocks at the Bloomington Crushed Stone and Sieboldt quarries.

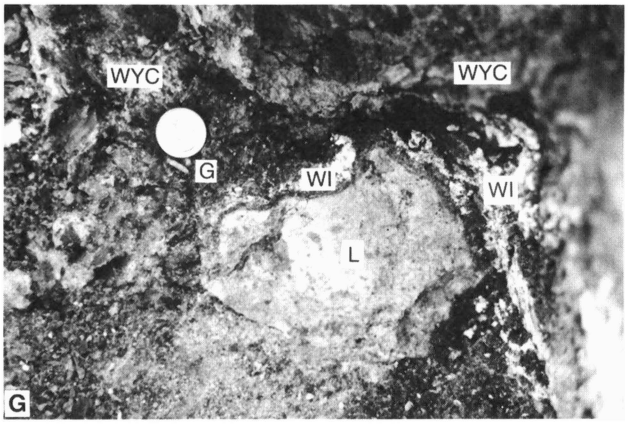

3G. Limestone "L" with dark crust of gypsum "G" and white indianaite "WI" from SQ. Surrounding material is waxy yellow gypsiferous clay "WYC." U.S. quarter for scale.

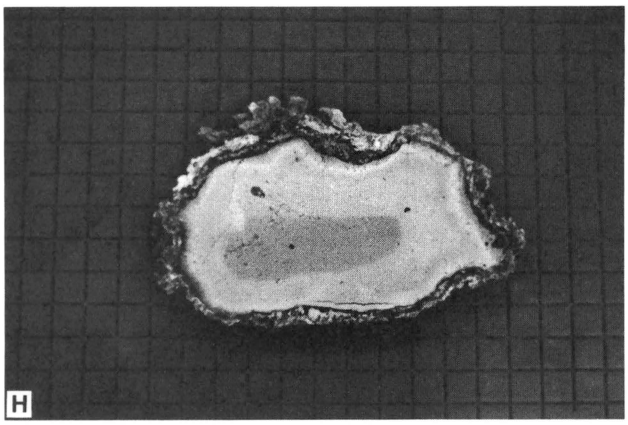

3H. Slab of limestone from a sample of the upper Paoli Formation at SQ. The sample was completely enclosed in waxy yellow gypsiferous clay. Note the concentric alteration haloes of the core limestone, the scalloped outline, and the dark gypsum crust that is coated with white hydrobasaluminite, especially on the top of the sample. Note the radiating gypsum crystals on the top of the sample. Background grid is 1.25 cm^2.

Figure 3. (cont.) Photographs showing relationships of indianaite to host rocks at the Bloomington Crushed Stone and Sieboldt quarries.

The geology at BCS suggested that indianaite should occur at the same stratigraphic interval at the Sieboldt Quarry located in the NE¼ SE¼ section 11, T. 6 N., R. 2 W., Lawrence County, Indiana. Indeed, indianaite is developed at the same horizon at SQ. The upper surface of the Paoli Formation at SQ is pitted by dissolution to depths of 50 cm. Friable grayish orange (10YR7/4) limestone as thick as 10 cm is common at the contact but not always present. The entire limestone surface is coated with 0.5-1 cm of selenite gypsum, which is itself coated with a 1-3 cm thick, white (5B9/1) crust (fig. 3F, G, H). A few white (N9) veins extend into the overlying clay as far as 60 cm above the limestone contact. Nearly all of the white material, however, occurs within 10 cm of the limestone contact. The white mineralization and gypsum are overlain upward by the following: as much as 20 cm of waxy moderate yellowish brown (10 YR 5/4) pyrolusite-stained clay containing radiating clusters of selenite gypsum as large as 5 cm in diameter; 30 cm of waxy, moderate brown (5YR4/4), pyrolusitic clay; 60 cm of dark yellowish-orange (10YR6/6), strongly rooted, clayey, weathered sandstone; 30 cm of strongly rooted, mottled, moderate reddish brown (10R4/6) and pale yellowish brown (10YR6/2), massive clay; and 30-100 cm of moderate yellowish-brown (10YR5/4) topsoil (fig. 3F).

The exposure at SQ is a remnant of a hill capped by the Bethel Formation, which has since been quarried away. A stockpile of the stripped Bethel Formation at the quarry shows that in the SQ area the unit contains approximately 60 cm of FeS-rich, clayey, sandstone and an unknown thickness of dark-gray, FeS-rich shale. Fragments of coal were found in the stockpile. Thin coal is common in the Bethel Formation (Kissling, 1967; Shaver and others, 1986). The mine supervisor recollects that the original Bethel Formation sequence at SQ was sandstone-coal-shale from bottom to top. Cores with file numbers SDH-341 (section 29, T6N, R2W, Lawrence County) and SDH-672 (section 22, T7N, R2W, Monroe County) at the Indiana Geological Survey Core Library show the base of the Bethel Formation in the vicinity of SQ consists of 75-100 cm of clayey, medium-grained, quartz sandstone (see figure 1 for core locations). Given that the base of the Bethel Formation at SQ is sandstone, the fact that as much as 50 cm of waxy clay occurs *below* the weathered sandstone at the quarry is pertinent to this discussion.

X-ray Diffraction

X-ray diffraction results from the BCS and SQ sample profiles show that the mineralogy of the indianaite substrate and the mineralogy of the weathered Bethel Formation overburden are similar at both localities. Indianaite mineralogy, however, is different at the two localities.

At BCS, the indianaite substrate is made of calcite with minor quartz. The indianaite zone contains halloysite (10Å) and accessory goethite, gibbsite, and pyrolusite (fig. 4A). Where present, gibbsite occurs adjacent to the carbonate substrate. Basal sandstone in the Bethel Formation contains quartz and minor well-crystallized kaolinite, and the lower gray shale contains quartz, poorly crystallized kaolinite, illite/mica, and minor smectite. Yellow, weathered shale above the gray shale is indistinguishable in bulk mineralogy from the gray shale. Yellow joint filling in the gray shale consists of the same clay mixture as the shale with minor quartz and abundant Fe-sulfates (mostly jarosite).

At SQ, the indianaite substrate is calcite with minor quartz. White clay identified in the field at SQ is hydrobasaluminite, basaluminite, gypsum, and minor gibbsite and halloysite (fig. 4B). White veins extending into the base of the weathered sandstone exhibit weak gibbsite and halloysite (10Å) reflections superimposed on a strong background with broad reflection bands at 22-30 and 34-42 degrees 2θ indicative of allophane (fig. 4C).

The lower, waxy, yellow, gypsiferous clay contains kaolinite/halloysite (7Å), halloysite (10Å), allophane, and small amounts of gibbsite, smectite, and quartz. The waxy, pyrolusitic clay contains quartz, kaolinite/halloysite (7Å), halloysite (10Å), allophane, smectite, and no gibbsite. Mineralogy of the weathered sandstone is dominated by quartz and contains minor smectite, mica, halloysite (10Å), kaolinite/halloysite (7Å), and allophane. The uppermost mottled zone contains abundant quartz with accessory kaolinite, illite/mica, and smectite. Pure allophane and halloysite (10Å) occur at GMR and the Stanford, Kentucky halloysite occurrence (Ettensohn and Bayan, 1990) and provided reference materials for comparison to the BCS and SQ indianaites (fig. 4C).

Scanning Electron Microscopy

Scanning electron microscopy results from BCS and SQ (figs. 5 and 6) clearly illustrate mineralogic similarities and differences of the deposits as well as textural evidence useful in interpretation of reactions relating to indianaite genesis.

Bethel shales and sandstones at BCS and SQ vary directly in their degree of textural and mineral alteration with the amount of weathering the rock has undergone, as shown by color and plant activity (yellow/rooted = more weathered; gray/not rooted = less weathered). Less weathered shale contains well-preserved, compactional fabric, mildly to moderately etched feldspar and mica, pyrite framboids, and a lack of amorphous coatings (figs. 5A-B, 6A). Less weathered sandstones lack amorphous grain coatings, have moderately to strongly etched feldspar grains, and have pore space commonly filled with well-crystallized kaolinite, pyrite, Fe-oxyhydroxide, and quartz overgrowths (figs. 5C, 6B). Weathered shale contains no pyrite but does have abundant Fe-oxyhydroxide and amorphous material, and the compactional swirl texture is randomized by plant root activity (fig. 6C). Weathered sandstone contains strongly etched feldspar, abundant pore-filling elongate halloysite and amorphous material, and no pyrite. Otherwise the mineralogy of the weathered sandstone is the same as less weathered sandstone (figs. 5D-E, 6D-F). Waxy clays below the weathered sandstone at SQ lack observable detrital fabric and are made mostly of allophane (fig. 6G-I). Waxy clays also contain minor quartz, gypsum, barite, and smectite (fig. 6J). Halloysite identified by XRD probably occurs as irregular bumps on the allophane (fig. 6H-I). Kaolinite cannot be identified in the waxy clays although a 7Å peak suggestive of kaolinite and/or halloysite (7Å) was identified by XRD (fig. 4B). Because

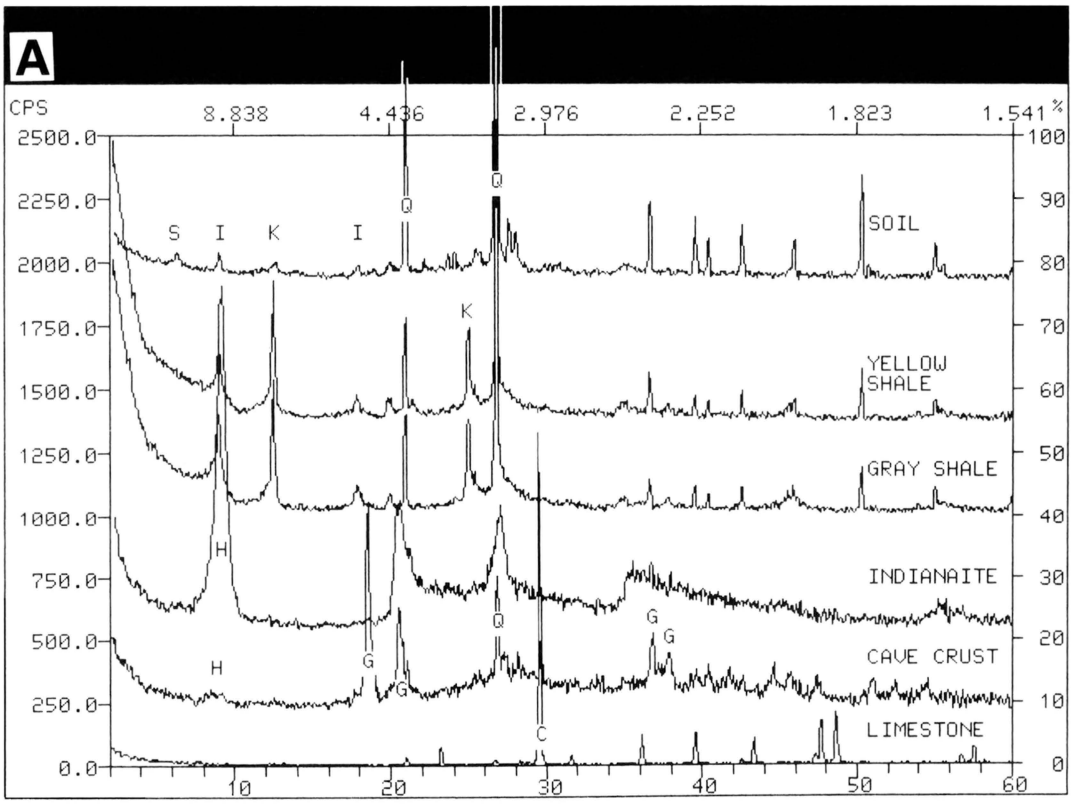

4A. Summary of diffraction results from BCS.

Figure 4. Summary of X-ray diffraction results. Scans are arranged stratigraphically. Sample labels on the scans correspond to figure 3. Peak labels include: Q = quartz, I = illite, S = smectite, K = kaolinite, H = halloysite, G = gibbsite, C = calcite, HYB = hydrobasaluminite, B = basaluminite, GYP = gypsum.

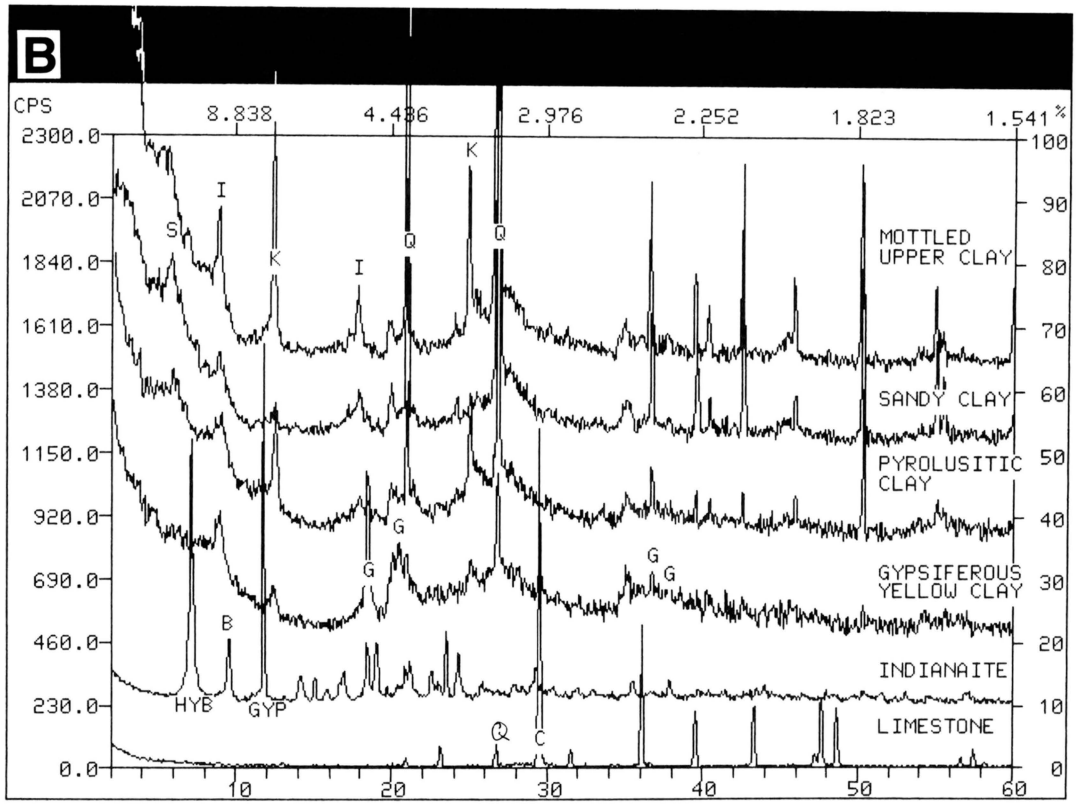

4B. Summary of diffraction results from SQ.

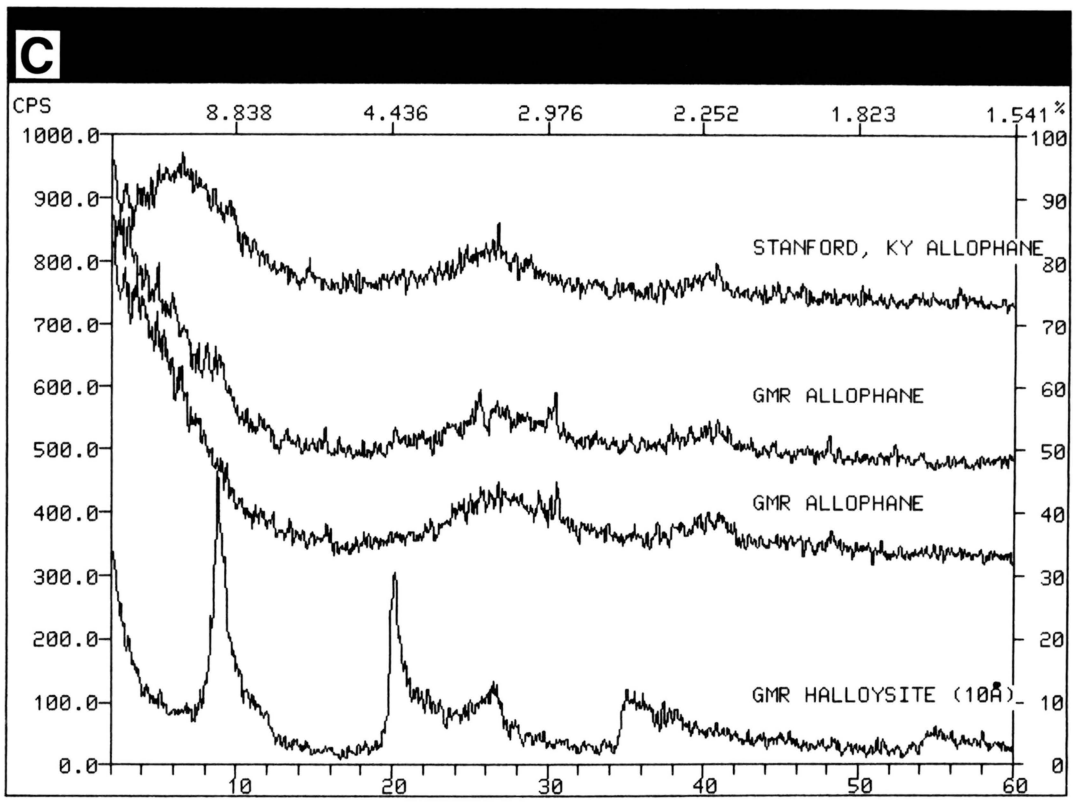

4C. Diffraction profiles for allophane and halloysite (10Å) from Stanford, Kentucky and GMR.

Figure 4. (cont.) Summary of X-ray diffraction results. Scans are arranged stratigraphically. Sample labels on the scans correspond to figure 3. Peak labels include: Q = quartz, I = illite, S = smectite, K = kaolinite, H = halloysite, G = gibbsite, C = calcite, HYB = hydrobasaluminite, B = basaluminite, GYP = gypsum.

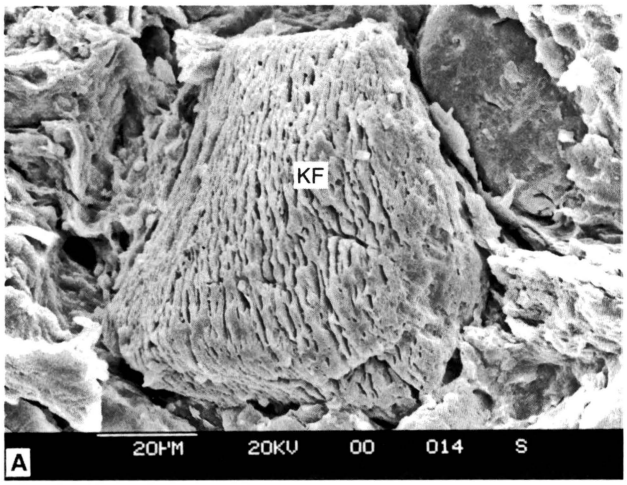

5A. Moderately etched potassium feldspar grain in gray Bethel Formation shale.

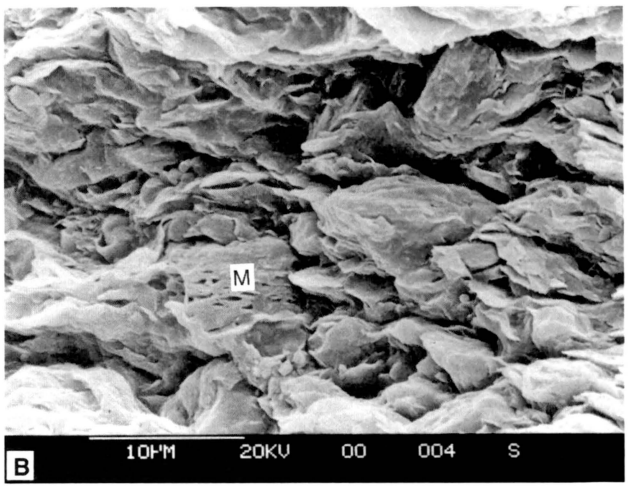

5B. Degraded muscovite grain "M" anastomosed by matrix composed of illite and kaolinite in gray Bethel Formation shale.

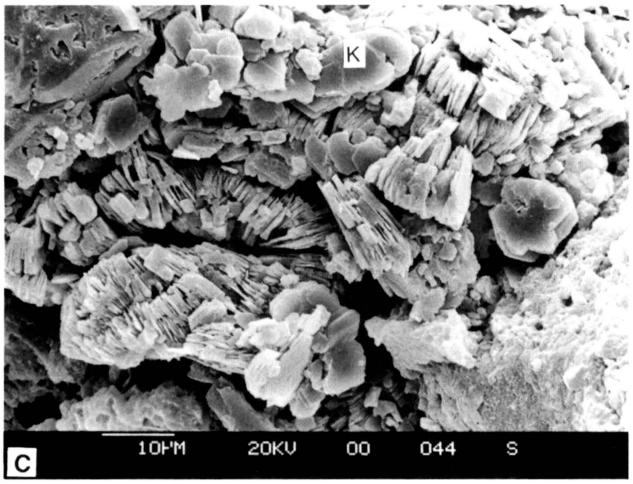

5C. Kaolinite pore-fill in gray sandstone from the basal Bethel Formation.

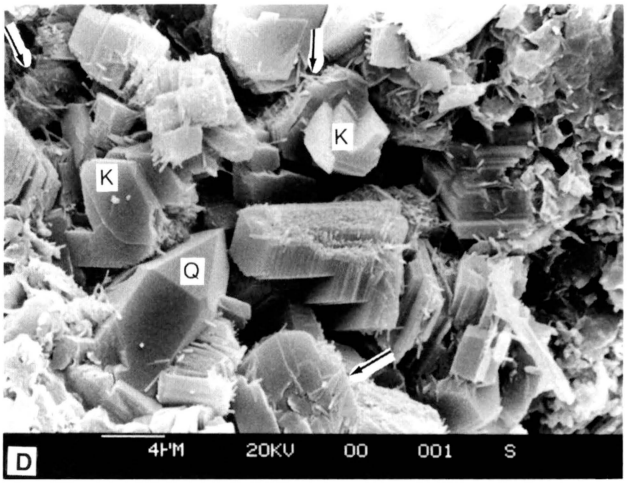

5D. Kaolinite and quartz pore-fill in yellow sandstone from the base of the Bethel Formation. Elongate halloysite shown forming from kaolinite crystals at arrows; it occurs as randomly distributed discrete particles in contrast to its globular occurrence in figure 5E-K.

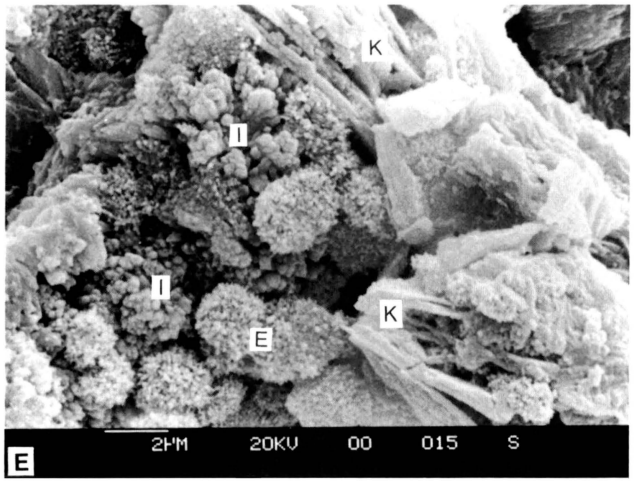

5E. Elongate halloysite lepispheres intergrown with globular iron oxyhydroxide and kaolinite in the base of the lower Bethel Formation sandstone.

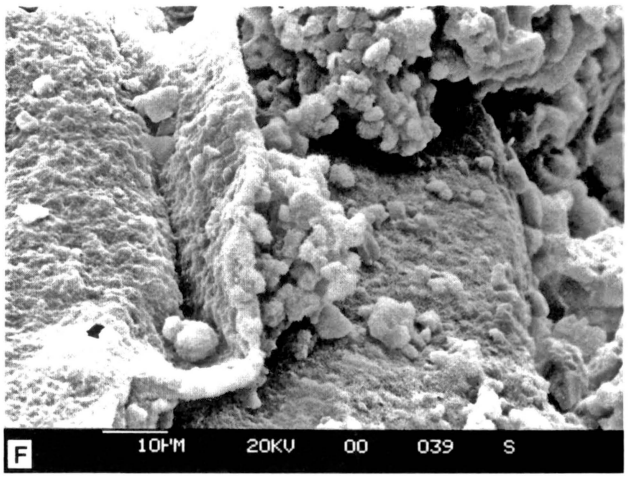

5F. Elongate halloysite coating the surface of folded allophane in the indianaite layer.

Figure 5. Scanning electron micrographs from the indianaite zone and surrounding materials at the Bloomington Crushed Stone quarry. Q = quartz, KF = potassium feldspar, K = kaolinite, E = elongate halloysite, I = iron oxyhydroxide, A = allophane. Sample identifications follow figures 3 and 4.

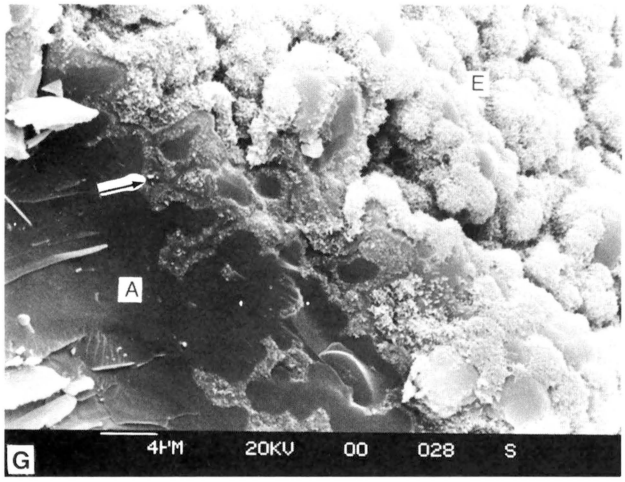

5G. Elongate halloysite coating the mammillary surface of allophane in the indianaite layer. Overgrowth of an early elongate halloysite coating by allophane (arrow) is apparent in the cross section provided by the broken surface.

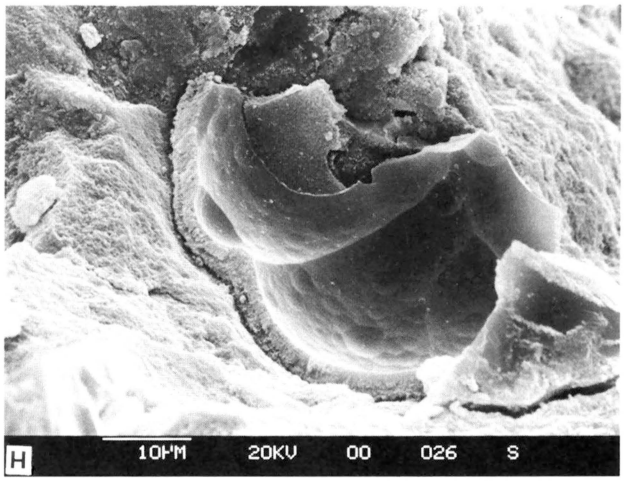

5H. Botryoidal elongate halloysite from the indianaite layer separated from an allophane substrate forming a clean mold of the allophane surface. Host material is coalesced, elongate-halloysite lepispheres.

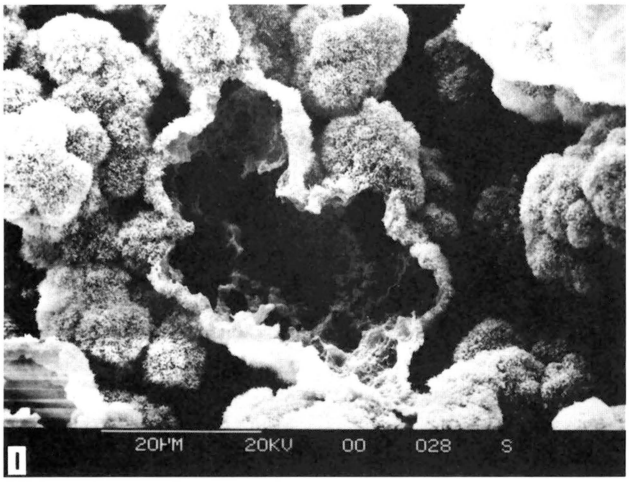

5I. Mammillary shell of halloysite remaining after substrate allophane dissolution (from cave fill).

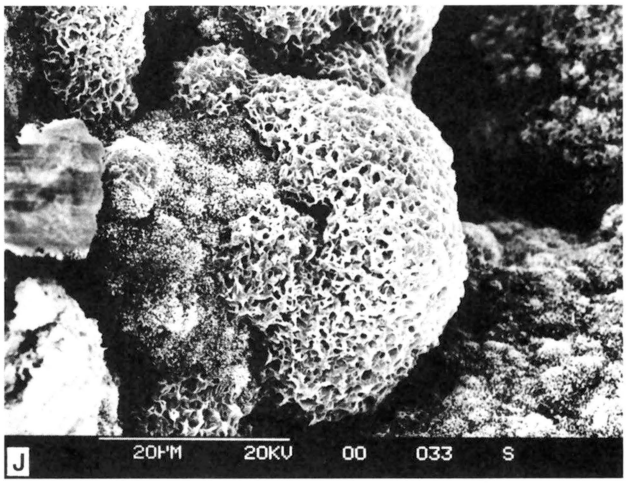

5J. Lepispheres of halloysite and smectite coating allophane substrate (from cave fill).

Figure 5. (cont.) Scanning electron micrographs from the indianaite zone and surrounding materials at the Bloomington Crushed Stone quarry. Q = quartz, KF = potassium feldspar, K = kaolinite, E = elongate halloysite, I = iron oxyhydroxide, A = allophane. Sample identifications follow figures 3 and 4.

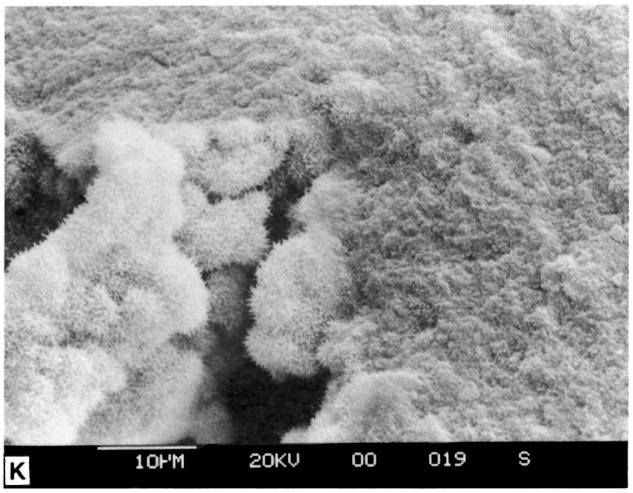

5K. Elongate halloysite lepispheres in void in porcelaneous indianaite is made up of coalesced elongate halloysite lepispheres.

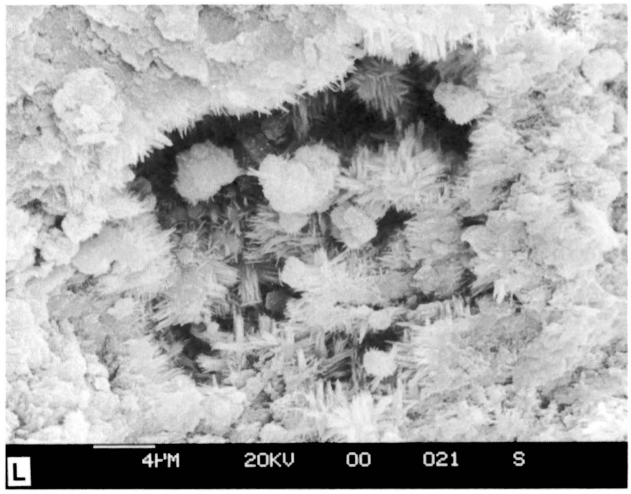

5L. Globular and acicular iron oxyhydroxide from below the indianaite layer.

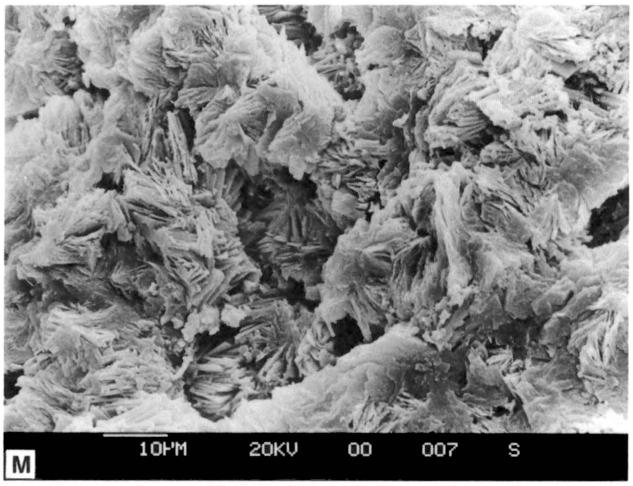

5M. Gibbsite pseudomorphously replacing hydrobasaluminite rosettes from adjacent to the carbonate substrate.

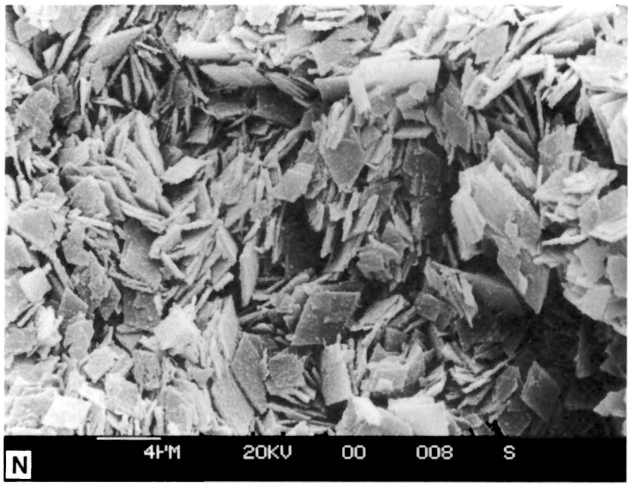

5N. Gibbsite pseudomorphously replacing hydrobasaluminite plates from cave surface crust.

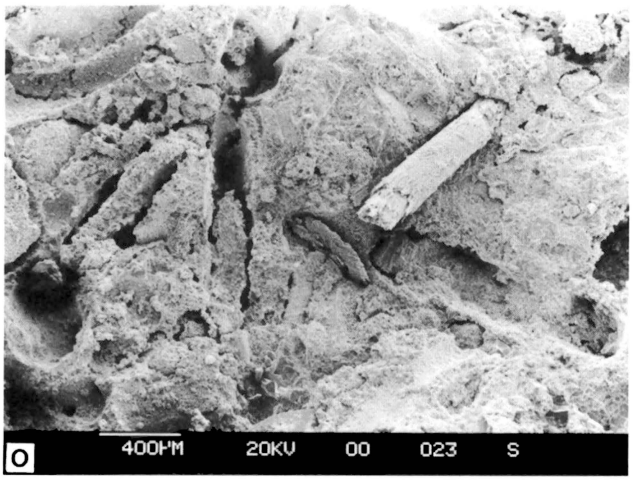

5O. Root casts and molds in the friable limestone.

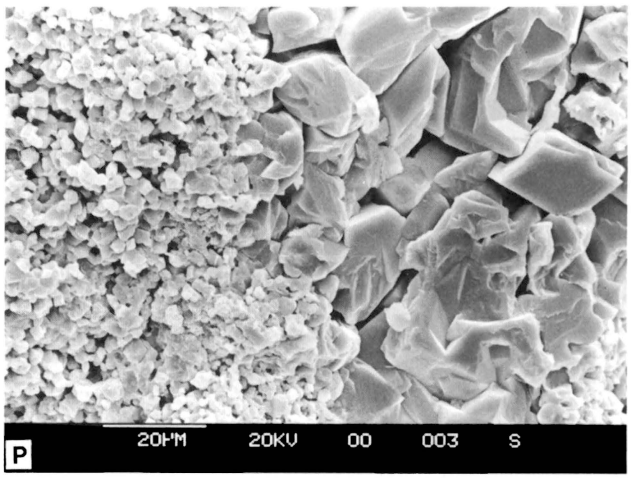

5P. Detail of calcite in the friable limestone showing enhanced porosity.

Figure 5. (cont.) Scanning electron micrographs from the indianaite zone and surrounding materials at the Bloomington Crushed Stone quarry. Q = quartz, KF = potassium feldspar, K = kaolinite, E = elongate halloysite, I = iron oxyhydroxide, A = allophane. Sample identifications follow figures 3 and 4.

of rooting, pores abound in the waxy clay and are lined with botryoidal allophane that is commonly laminated (fig. 6H). The bumpy surface of the allophane (fig. 6I) is similar in appearance to well-developed, elongate BCS halloysite, which is also developed on allophane (fig. 5F-J). Though not appearing as such in outcrop, the waxy zones at SQ are more like indianaite in mineral content and texture than altered formation clay. White indianaite at BCS is composed of allophane, elongate halloysite, gibbsite, and Fe-Mn-oxyhydroxide (fig. 5F-N). Vertical changes through the indianaite include allophane and elongate halloysite at the top; pure, globular, elongate halloysite in the middle (similar to that described by Diamond and Bloor, 1970); and gibbsite adjacent to the limestone substrate. These changes are mimicked in the cave fillings from center to wall. Hydrobasaluminite was identified in the field as indianaite at SQ (fig. 6K-L). Hydrobasaluminite occurs as well-formed, clean, rhomb-shaped plates and rosettes of plates. This morphology is the same as that of the gibbsite crust on the limestone substrate at BCS (fig. 5M-N). The friable limestone substrate of the indianaite at BCS and SQ is made of variable particle size anhedral calcite commonly containing root tubules, replaced roots, relict fossil fragments, and relict ooids (figs. 5O-P, 6M-N).

Petrography

To adequately study mineral intergrowths at the limestone/indianaite interface, thin sections were made for petrographic analysis. Thin sections of SQ materials were prepared from samples similar to that shown in figure 3H in which the gypsum crust is well attached to the limestone substrate. Samples from BCS graded from hard to friable limestone and do not include macroscopically visible indianaite. All thin sections of the limestone contact contain gypsum as optically continuous microfracture filling or calcite replacement (fig. 7A-C). Typically, the hard limestone substrate is etched near the contact to yield a porous zone a few millimeters thick. At SQ, the pores in the limestone are progressively enlarged and filled with gypsum and/or hydrobasaluminite until the calcite is completely replaced (fig. 7B-C). Rarely, halloysite (as minute nodules) and allophane (as laminated yellow pore-linings) occur in the gypsum/hydrobasaluminite crust (fig. 7D-E). Allophane coats irregularly shaped pores similar in shape to pedotubules identified by SEM (fig. 6M). At BCS, gypsum fills pore spaces adjacent to hard limestone with a framework of relict calcite grains making up the friable limestone below the indianaite.

Thermal Analysis

Indianaite from BCS and SQ was analyzed by differential thermal analysis/thermal gravimetric analysis to support X-ray diffraction results and to better define relative amounts of allophane and halloysite (10Å) in the samples. Samples from GMR of pure hyaline allophane and very light green (10G8/2) halloysite (10Å) were analyzed to develop a method of quantification for each phase in the samples from BCS and SQ (fig. 8). Pure allophane dehydrates nearly completely over a temperature range of 50-250°C. Halloysite (10Å), however, loses half of its mass from 50-250°C (interlayer water) and the other half from 250-630°C (octahedral water). Assuming a mixture is composed only of allophane and halloysite (10Å), relative proportions of each phase can be obtained by using the steps outlined below. Mass loss from 250-630°C (halloysite octahedral water) is subtracted from the mass loss at 50-250°C, the remainder being the mass lost by allophane. The difference of the mass contained in allophane from the total mass loss is the water contained in halloysite (10Å). Halloysite (10Å) contains approximately 28 percent total moisture, and pure allophane samples from GMR were found to contain approximately 47.5 percent total moisture using the sample preparation described above. Using the mass of moisture measured by thermal gravimetry and these assumed moisture contents for halloysite (10Å) and allophane, a simple proportion was used to calculate the total mass of each phase. The sum of the masses of both phases compared to the actual mass of sample analyzed provides an estimate of the reliability of the results. The calculations assume that the 250-630°C mass loss is entirely the result of halloysite dehydroxylation (no kaolinite) and the 50-250°C mass loss is entirely caused by allophane dehydration and halloysite (10Å) interlayer water loss with no contribution from smectite. These assumptions are supported by electron microscopy which shows that smectite and kaolinite are minor components of the indianaite at BCS and SQ.

BCS indianaite was determined by this analysis to be made of 51.9 percent halloysite (10Å) and 43.8 percent allophane (halloysite 10Å : allophane mass ratio = 1.18). SQ waxy yellow clay is made of 35.8 percent halloysite (10Å) and 42.1 percent allophane (halloysite 10Å : allophane mass ratio = 0.85). SQ waxy pyrolusite-stained clay is made of 26.2 percent halloysite (10Å) and 49.8 percent allophane (halloysite 10Å : allophane mass ratio = 0.53). This analysis shows that halloysite (10Å) content increases toward the limestone interface at SQ and that the material in contact with the limestone at BCS contains more halloysite (10Å) than the waxy clays at SQ. Inert material in the waxy clays at SQ should be approximately 25 percent by weight as suggested by the totals for allophane and halloysite (10Å) in this analysis. This value is supported by and in agreement with XRD and SEM observations that show significant amounts of quartz in the waxy clays, probably from the base of the weathered sandstone.

DISCUSSION

Comparison of Indianaite Occurrences

Indianaite deposits at BCS and SQ are similar, although they differ in some important aspects. The BCS indianaite deposit is planar and underlain by limestone with enlarged joints,

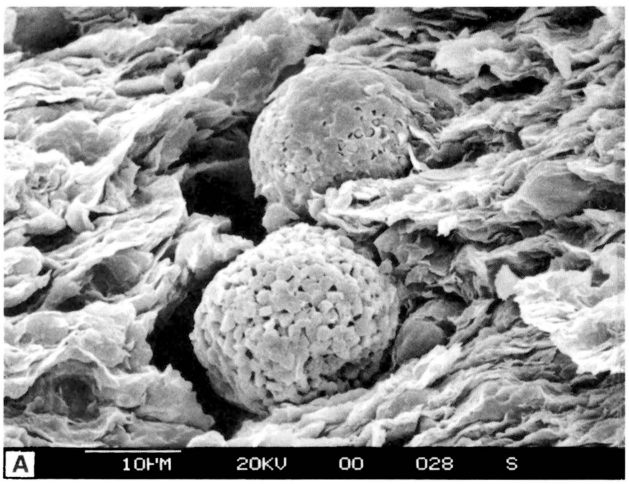

6A. Pyrite framboids anastomosed by clay from gray Bethel Formation shale stockpile (see text).

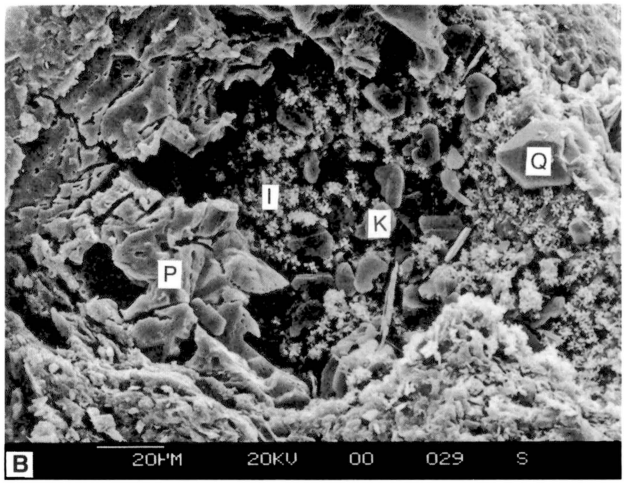

6B. Strongly etched plagioclase grain "P" in pyritic Bethel Formation sandstone from the shale stockpile. The core of the etched grain is filled with quartz, Fe-oxyhydroxide, and well-crystallized kaolinite.

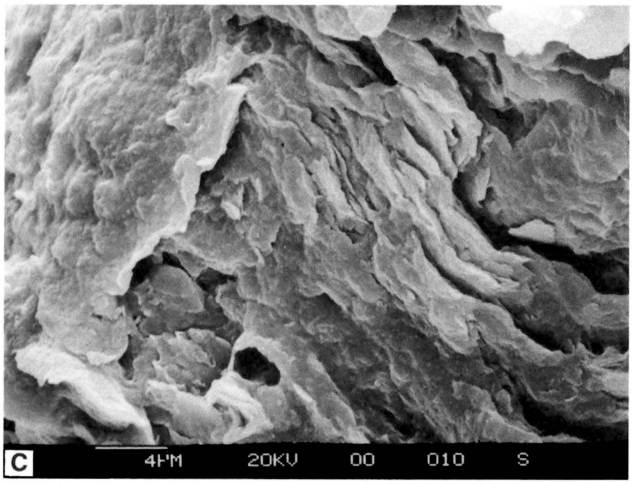

6C. Upper red/gray mottled clay showing compactional fabric truncated by a pedotubule with a surface coating of clay and allophane.

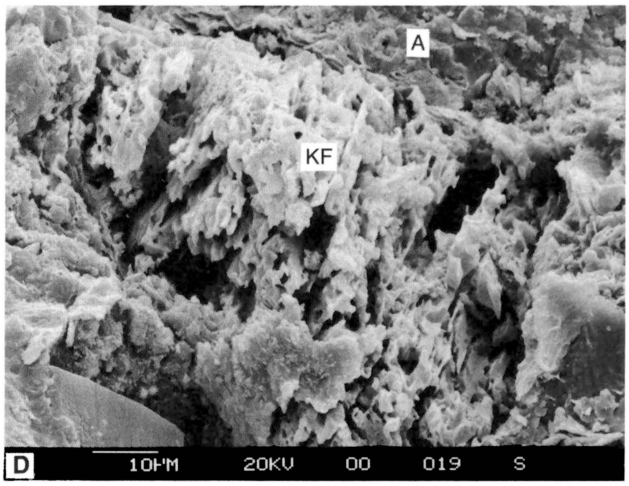

6D. Very strongly etched potassium feldspar grain in the weathered sandstone layer. Note quartz overgrowth in lower left and allophane pore-fill.

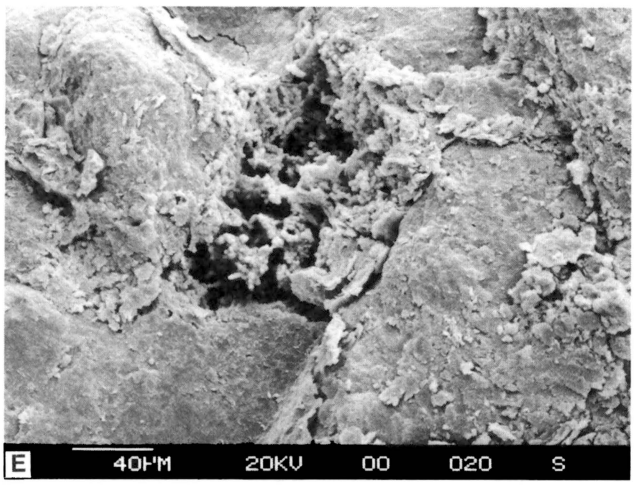

6E. Nearly completely dissolved potassium feldspar grain in the weathered sandstone layer with elongate halloysite lepispheres coating the relict feldspar and ridges of allophane.

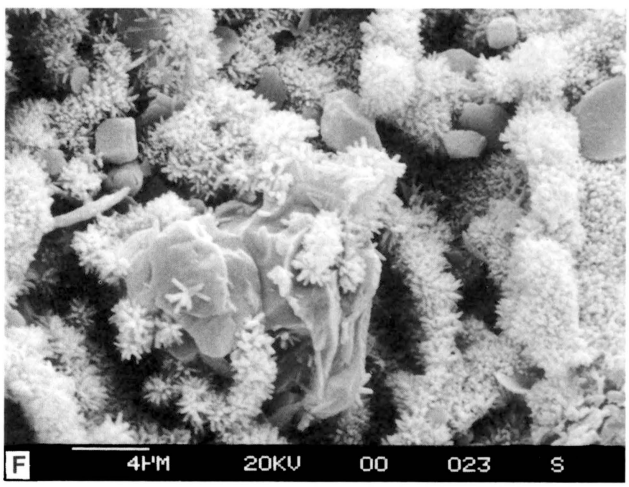

6F. Detail of E showing elongate halloysite lepispheres.

Figure 6. Scanning electron micrographs from the indianaite zone and associated materials at Sieboldt Quarry. Mineral labels are the same as in figure 5 and sample identifications follow figures 3 and 4.

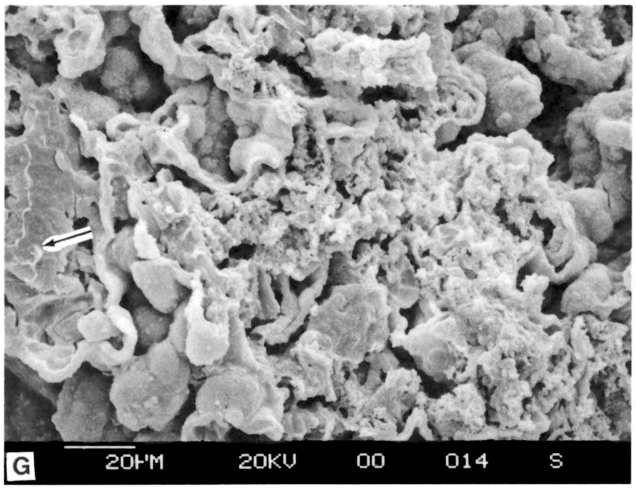

6G. General character of the waxy yellow gypsiferous clay. Botryoidal pore-lining allophane dominates the field of view. Minor smectite forms desiccation ridges (arrow).

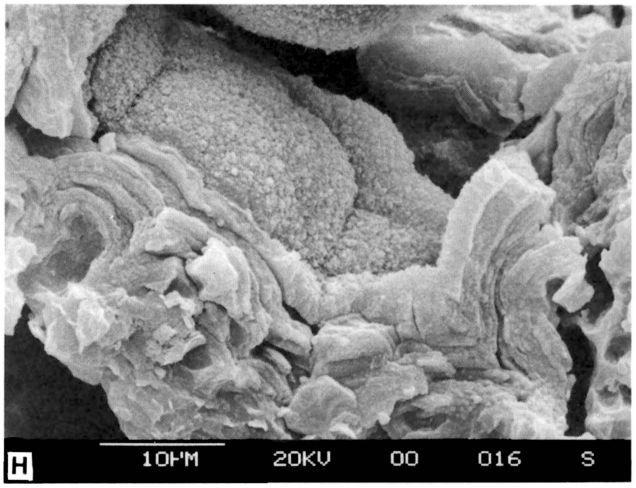

6H. Detail of G showing laminated botryoidal allophane with possible elongate halloysite nuclei covering the pore surface.

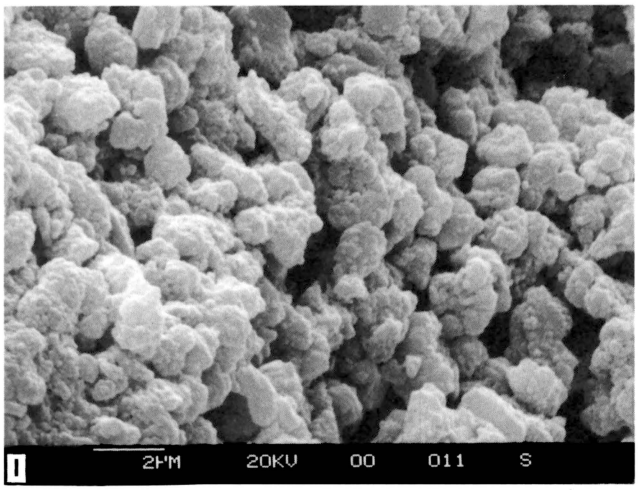

6I. Detail of a rough allophane surface in the waxy yellow gypsiferous clay. Individual nodes are made of coalesced spherical particles.

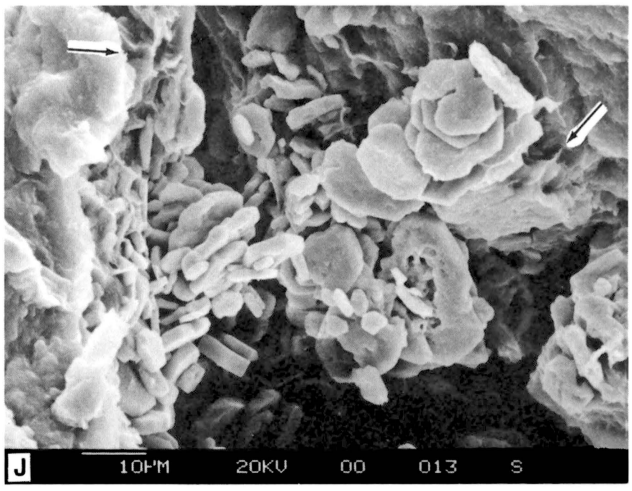

6J. Void in the waxy yellow gypsiferous clay filled with euhedral barite. Note minor smectite (arrows).

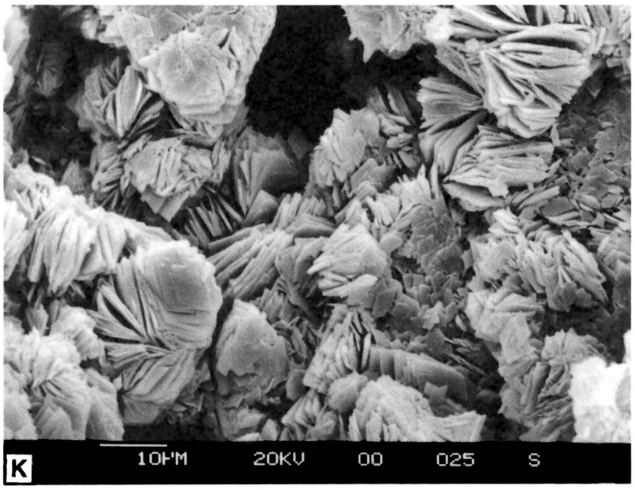

6K. Rosettes of hydrobasaluminite from above the gypsum crust on the substrate limestone. Compare with figure 5M.

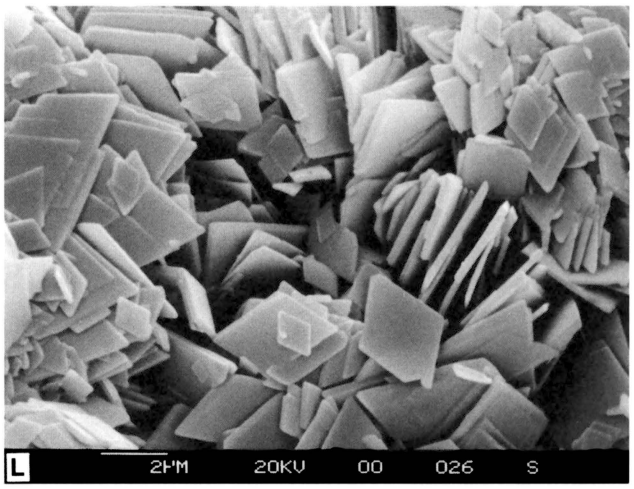

6L. Plates of hydrobasaluminite from the same horizon as K. Compare with figure 5N.

Figure 6. (cont.) Scanning electron micrographs from the indianaite zone and associated materials at Sieboldt Quarry. Mineral labels are the same as in figure 5 and sample identifications follow figures 3 and 4.

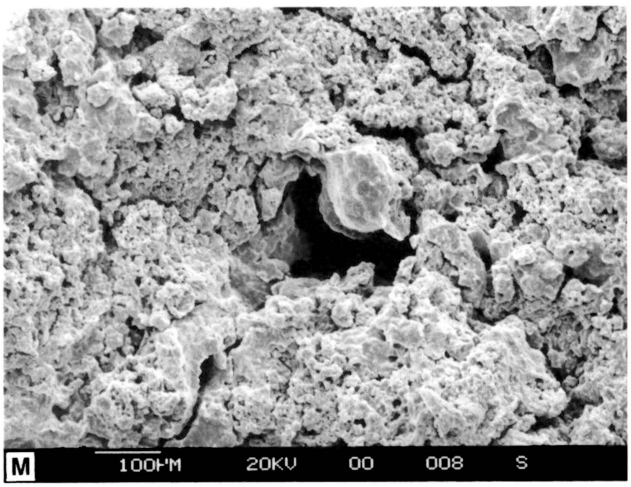

6M. Friable substrate limestone showing a cross section of a large pedotubule with smaller branching tubules in the surrounding clay.

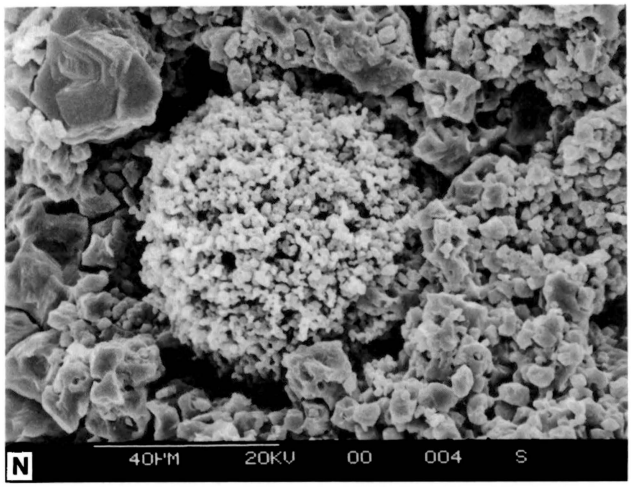

6N. Detail of a relic ooid from the friable limestone.

Figure 6. (cont.) Scanning electron micrographs from the indianaite zone and associated materials at Sieboldt Quarry. Mineral labels are the same as in figure 5 and sample identifications follow figures 3 and 4.

whereas the SQ deposit has wavy, gradational contacts and is underlain by limestone with few enlarged joints. Gypsum is rare at BCS and common at SQ. Bluish porcelaneous indianaite is common at BCS, and white powdery indianaite with yellow-brown waxy clay are common at SQ. A thick gray shale section penetrated by oxidized joints (channels of oxygenated and acidified fluid flow) above the BCS indianaite is overlain by a yellow/tan section similar in thickness to that at SQ, but no gray shale occurs above the indianaite at SQ.

The GMR deposit is similar to indianaite at SQ and BCS as shown by the reports of Cox (1875), Logan (1922a, b), Reis (1922), Callaghan (1948), Sunderman (1963), and Dombrowski and others (1988). A spectrum of indianaite types occur at GMR including: nodular porcelaneous indianaite like that at BCS; mahogany clay identical to the waxy clays at SQ; powdery, white, Al-sulfate-rich indianaite similar to the SQ material; yellow to green translucent pods of allophane; plastic white to yellow kaolin; and dark greenish-gray, pyritic indianaite, that occurs irregularly along the base of the mineralized zone. Overburden of the indianaite is as thick as 35 m and is comprised of medium- to coarse-grained quartz sandstone cemented with Fe-Mn oxyhydroxides and quartz overgrowths. Well-crystallized kaolinite is a common pore filling, and relic feldspars and muscovite have been identified and were probably important components in the original sediment (as much as 15 percent). Blocks of the sandstone as large as several meters in maximum dimension are completely or partially enclosed in the indianaite. Indianaite is underlain by several rock types at GMR. Drill hole descriptions given in plate 1 of the report by Callaghan (1948) include 23 drill holes for which the substrate material of the indianaite was identified. Of these, 13 had limestone, 5 had shale, and 5 had sandstone below the indianaite. Indianaite was thickest (as thick as 5 m) where the substrate was shale or sandstone; but where limestone was the substrate, the indianaite was less than 2.5 m thick. This implies that where shale or sandstone are the substrate of thick indianaite, the limestone was removed by indianaite replacement.

Except for the thicknesses of indianaite, the GMR, BCS, and SQ deposits are similar. In all three cases, the indianaite occurs above and in contact with limestone and below weathered siliciclastic rock which contains abundant FeS where unweathered. Where the limestone was completely replaced by indianaite at GMR the deposit is bounded above and below by siliciclastic rocks.

Textures and Mineral Reactions

Weathering and oxidation of siliciclastic sediments above indianaite at BCS, SQ, and GMR is concomitant with changes in constituent mineralogy and mineral morphology. Textures indicate reaction of the minerals with aqueous fluid (dissolution). Textures in the indianaite and upper few centimeters of limestone suggest precipitation of minerals from aqueous solution.

Pyrite was identified in unweathered sediments above the indianaite at BCS and SQ (fig. 6A) and only Fe-oxyhydroxides and minor jarosite in the weathered sediments at these localities. Callaghan (1948) reports that the Mansfield Formation sandstone at GMR contains abundant Fe-oxyhydroxides and no pyrite. Cores of Mansfield Formation sandstone available at the Indiana Geological Survey Core Library, however, show that the sandstone is typically pyritic in the subsurface. This evidence indicates that pyrite and/or marcasite existed at BCS, SQ, and GMR and oxidized to Fe-oxyhydroxides and sulfuric acid by reaction with surface water containing dissolved oxygen.

1) $4FeS_2 + 15O_2 + 14H_2O \rightarrow 8H_2SO_4 + 4Fe(OH)_3$

This summary reaction for FeS weathering (see Stumm and Morgan, 1981, for step reactions) shows the net production of sulfuric acid. FeS oxidation is strongly catalyzed by activity of the iron and sulfur oxidizing bacteria *Ferrobacillus sp.* and *Thiobacillus sp.* (Barnes and Clark, 1964; Etherington, 1975; Stumm and Morgan, 1981; Krause, 1989). Logan (1922b) documented the presence of these bacteria at GMR. Oxygenated water for the reaction is provided by meteoric water. High oxygen content in the water is maintained by diffusion of O_2 through the soil atmosphere during downward migration of the water to the water table (Etherington, 1975, p. 126; Stolzy, 1974).

K-feldspar, plagioclase, and muscovite detritus of Bethel sediments are etched at BCS and SQ (figs. 5A, B; 6B, D, E, F) similar to those reported by Berner and Holdren (1979). Dombrowski and others (1989) identified similar textures in feldspars in sandstone from GMR. Very well crystallized, authigenic kaolinite converts to halloysite in weathered material (fig. 5C, D). Grains of each of these minerals that are the most strongly altered occur in the most weathered sediments where sulfuric acid production probably occurred. Based on this evidence, sulfuric acid is a reactant in the following reactions except in reaction **2e** where the sulfuric acid catalyzes the conversion of kaolinite to halloysite.

2a) $KAlSi_3O_8$ (K-feldspar) $+ 2H_2SO_4 + 4H_2O \rightarrow K^+ + Al^{3+} + 2(SO_4)^{2-} + 3H_4SiO_4$

2b) $NaAlSi_3O_8$ (albite) $+ 2H_2SO_4 + 4H_2O \rightarrow Na^+ + Al^{3+} + 2(SO_4)^{2-} + 3H_4SiO_4$

2c) $CaAl_2Si_2O_8$ (anorthite) $+ 4H_2SO_4 \rightarrow Ca^{2+} + 2Al^{3+} + 4(SO_4)^{2-} + 2H_4SiO_4$

2d) $KAl_3Si_3O_{10}(OH)_2$ (muscovite) $+ 5H_2SO_4 \rightarrow K^+ + 3Al^{3+} + 5(SO_4)^{2-} + 3H_4SiO_4$

2e) $Al_2Si_2O_5(OH)_4$ (kaolinite) $+ 2H_2O \rightarrow Al_2Si_2O_5(OH)_4 \cdot 2H_2O$ (halloysite 10Å)

2f) $2Ca_5(PO_4)_3(OH)$ (apatite) $+ H_2SO_4 \rightarrow 10Ca^{2+} + 6(PO_4)^{3-} + (SO_4)^{2-} + H_2O$

No dissolution textures in apatite supporting reaction **2f** were observed, but the occurrence of crandallite (Sunderman, 1963), kingite (Robert J. Pruett, 1989, personal communication), and allophane-evansite (Ross and Kerr, 1935; Callaghan, 1948) in the indianaite at GMR require some such source of phosphate. Silica released by these dissolution reactions is unstable in low pH environments (Hem, 1959) and probably contributed to quartz overgrowths observed in the sandstones at BCS, SQ, and GMR.

Limestone replacement textures (figs. 3, 7) indicate interaction between fluid and carbonate substrate. Sunderman (1963, plates 3 and 5) identified identical replacement textures in GMR and nearby deposits, but he did not give the interpretations that follow here in that study. Minerals replacing calcite in the limestone give direct evidence of the composition of the fluid which interacted with the limestone to yield them. Most apparent in figures 7A through 7C is the replacement of calcite in the limestone by gypsum.

3) $H_2SO_4 + CaCO_3$ (calcite) $+ H_2O \rightarrow CaSO_4 \cdot 2H_2O$ (gypsum) $+ CO_2$

Growth of gypsum is highly disruptive to surrounding materials (Dougherty and Barsotti, 1972; Quigley and Vogan, 1970) and may facilitate reaction of acid water with carbonate by fracturing and disruption of earlier-formed precipitates. Gypsum at the limestone contact below weathered siliciclastic rocks shows that sulfate-rich water interacted with the limestone, further supporting FeS weathering in the overlying rocks (reaction **1**).

Minerals embedded in and associated with the gypsum produced by reaction **3** are easily explained by precipitation of dissolved species resulting from the increase in pH caused by neutralization of sulfuric acid in reaction **3**. These minerals include allophane, hydrobasaluminite, Fe-oxyhydroxides (here simplified as goethite), Mn-oxyhydroxides (here simplified as pyrolusite), and possibly halloysite (10Å).

4a) $SiO_2aq + Al_2O_3aq + (OH)^- + H_2O \rightarrow (SiO_2)_{0.74\text{-}1.98}(Al_2O_3)(OH)_m \cdot nH_2O$ (allophane)

4b) $4Al^{3+} + (SO_4)^{2-} + 10(OH)^- + 36H_2O \rightarrow Al_4(SO_4)(OH)_{10} \cdot 36H_2O$ (hydrobasaluminite)

4c) $Fe^{3+} + 3(OH)^- \rightarrow Fe(OH)_3$ (goethite)

4d) $Mn^{2+} + 2(OH)^- + \frac{1}{2}O_2 \rightarrow MnO_2$ (pyrolusite) $+ H_2O$

4e) $2Al^{3+} + 2H_4SiO_4 + 6(OH)^- \rightarrow Al_2Si_2O_5(OH)_4 \cdot 2H_2O$ (halloysite 10Å)

Minor smectite in the waxy clays at SQ (fig. 6G) and cave fill at BCS (fig. 5J) probably also precipitated by a reaction similar to these but in neutral pH to alkaline environments close to the limestone (Chigara, 1990). Field evidence shows that these minerals occur at BCS and SQ where no overlying clay residuum existed before their emplacement, i.e., below sandstone in contact with limestone or in caves. Cationic species are carried to the precipitation site (reactions **3** and **4a - 4e**) from dissolution

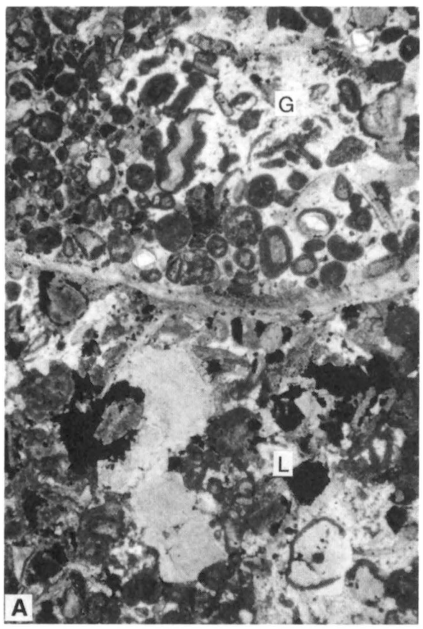

7A. Gypsum cemented/replaced limestone from the friable carbonate zone at BCS. Optically continuous gypsum is partially dissolved above a brachiopod fragment protecting gypsum below it from dissolution. [Crossed polars.]

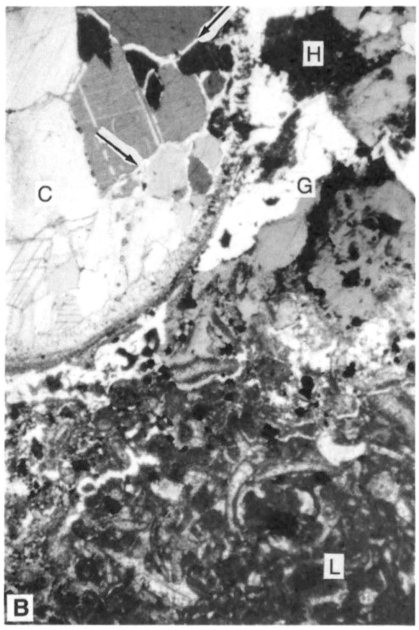

7B. Limestone contact at SQ. Gypsum and hydrobasaluminite replacing fine carbonate material has engulfed a large calcite-filled brachiopod. Gypsum has begun replacement of the spar along grain boundaries (arrows). The limestone substrate shows enhanced porosity near the gypsum interface and gypsum-filled fractures. [Crossed polars.]

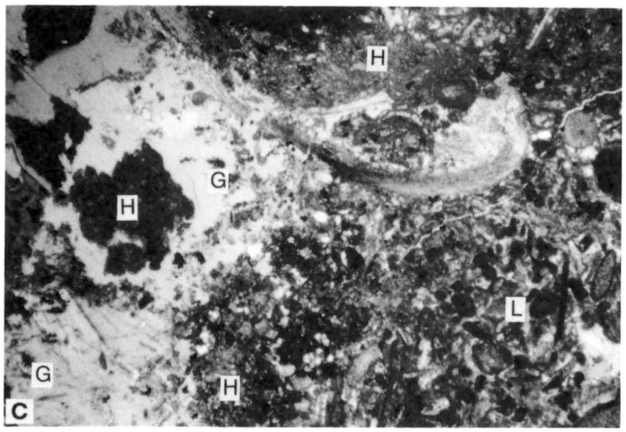

7C. Limestone contact at SQ. Dense limestone (lower right) shows enhanced porosity at the indianaite contact. The contact is mostly hydrobasaluminite with large gypsum grains further from the contact including hydrobasaluminite nodules. Note brachiopod partially isolated from the substrate limestone and enclosed in gypsum and hydrobasaluminite. A gypsum-filled fracture extends along the limestone contact through the friable carbonate zone. [Crossed polars.]

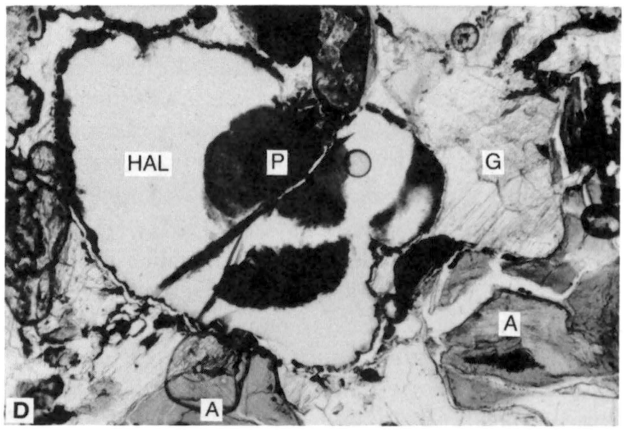

7D. Detail of a pyrolusite-stained halloysite nodule associated with gypsum, hydrobasaluminite, and allophane in the SQ basal indianaite. [Plane polarized light.]

Figure 7. Photomicrographs showing indianaite minerals and their relation to the substrate limestone. G = gypsum, H = hydrobasaluminite, C = calcite, A = allophane, P = pyrolusite, HAL = halloysite, L = limestone. The long dimension of each photomicrograph is 8 mm.

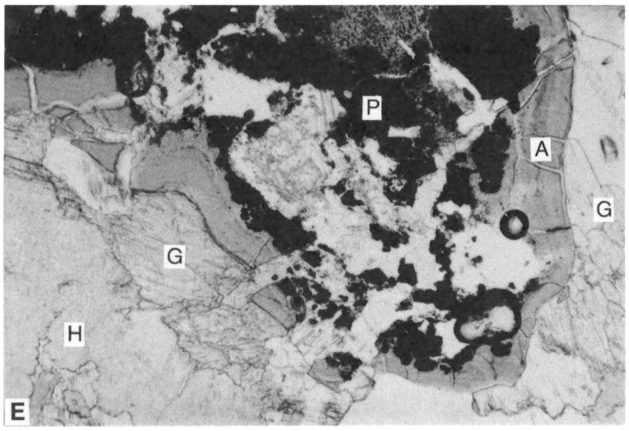

7E. Detail of a pyrolusite-, gypsum-, halloysite- and allophane-filled void in the host hydrobasaluminite and gypsum of the basal indianaite at SQ. Fractures in the allophane are filled with gypsum. [Plane polarized light.]

Figure 7. (cont.) Photomicrographs showing indianaite minerals and their relation to the substrate limestone. G = gypsum, H = hydrobasaluminite, C = calcite, A = allophane, P = pyrolusite, HAL = halloysite, L = limestone. The long dimension of each photomicrograph is 8 mm.

sites in the overlying rock (reactions **2a - 2f**) by downward migrating meteoric water. *In situ* alteration of aluminous residuum developed on limestone is therefore unnecessary in formation of indianaite. Solubility of Al and silica are strongly pH dependent (fig. 9). Published ground-water analyses from carbonate terrains and coal mine spoils illustrate the naturally occurring variations in aluminum and silica in high-pH waters versus low-pH waters and suggest general compositional limits for the acid water involved in indianaite formation and the effect of neutralization of these waters (fig. 9). Aluminum solubility decreases abruptly at pH = 4.0 (Mason, 1952) (fig. 9A). Few of the natural waters compiled from the literature had pH values between 3.7 and 5.3 suggesting the natural predominance of the carbonate and sulfide buffers in regulating oxygenated groundwater pH's. Silica data compiled from the literature is confined almost entirely to the pH range 5.0-9.5. Data in this range show increased solubility of silica with rising pH, and nearly all the data fall in the soluble region for silica calculated by Mason (1952) (fig. 9B). Iron and manganese solubility (important in reactions **4c** and **4d**) are strongly dependent on Eh and pH (fig. 10). A distinct decrease in dissolved iron and manganese with increasing pH is shown on the diagrams. These data suggest that increase in pH by reaction of acidic water with limestone can force precipitation of iron and manganese and produce the limonite and pyrolusite common in indianaite occurrences.

Scanning electron micrographs show textures suggesting that primary precipitates at the carbonate interface are transformed to secondary indianaite minerals. Allophane in samples from BCS and SQ are commonly coated by halloysite. Material from BCS identified by XRD as gibbsite has identical morphology to hydrobasaluminite at SQ, although the gibbsite had a rough, altered appearance.

5a) $(SiO_2)_{0.74\text{-}1.98}(Al_2O_3)(OH)_2 \cdot nH_2O$ (allophane) $\pm$ xH_4SiO_4 $\pm$ yAl^{3+} $\rightarrow$ $zAl_2Si_2O_5(OH)_4 \cdot 2H_2O$ (halloysite 10Å)

5b) $Al_4(SO_4)(OH)_{10} \cdot 36H_2O$ (hydrobasaluminite) + $2(OH)^-$ $\rightarrow$ $4Al(OH)_3$ (gibbsite) + $(SO_4)^{2-}$ + $36H_2O$

These changes may be driven by the pH increase as fluids adjacent to the limestone equilibrate with calcite and cause pH increases as high as 8.5 (fig. 9A). Increased pH improves mobility of silica (Hem, 1959), which would allow migration of silica to or away from allophane as required for the formation of halloysite (10Å) in reaction **5a**. Growth of halloysite (10Å) may also be controlled by kinetic constraints preventing nucleation until allophane precipitates and forms a template for halloysite (10Å) growth (Steefel and van Cappellen, 1990). Wollast (1967) suggests that reaction of H_4SiO_4 with amorphous $Al(OH)_3$ is an important step in the conversion of feldspar to kaolinite, implying that aluminous, amorphous precipitates formed in indianaite as pH increases above 4.0 may convert to allophane and subsequently halloysite (10Å) only as fast as H_4SiO_4 is supplied for reaction (as in reaction **5a**). Halloysite (10Å) is stable to approximately pH = 7.0 in systems with low alkali metal concentrations (Merino and others, 1989). Marked increase in silica solubility above pH = 5.0 (fig. 9B) may allow removal of silica from the pH>5.0 site out of the system or to regions of allophane/halloysite (10Å) growth. Local removal of silica combined with further increasing pH, forces gibbsite stability (Dombrowski and others, 1989) and may be responsible for gibbsite in indianaite adjacent to limestone. Conversion of hydrobasaluminite to gibbsite occurs as pH values of 1.0-3.0 favorable for hydrobasaluminite precipitation rise adjacent to the limestone to values of 4.0-8.5 at which gibbsite is strongly supersaturated (Drever, 1988). Lowering of $(SO_4)^{2-}$ activity in the fluid by formation of gypsum may also cause hydrobasaluminite to release its relatively small sulfate content and pseudomorphously convert to gibbsite.

Origin of Indianaite

Field evidence, textures, and inferred reactions for BCS, SQ, and GMR indianaite and associated rocks support a concise model for the emplacement of indianaite (fig. 11).

1) Geologic conditions required for indianaite formation are as follows: the occurrence of feldspar and mica-bearing, FeS-rich, siliciclastic rock overlying carbonate rock; the vadose zone must extend through the siliciclastic unit and into at least the upper part of the carbonate unit; the siliciclastic unit must not contain enough carbonate to buffer the pH of the vadose water to values above the solubility break of aluminum (i.e.,

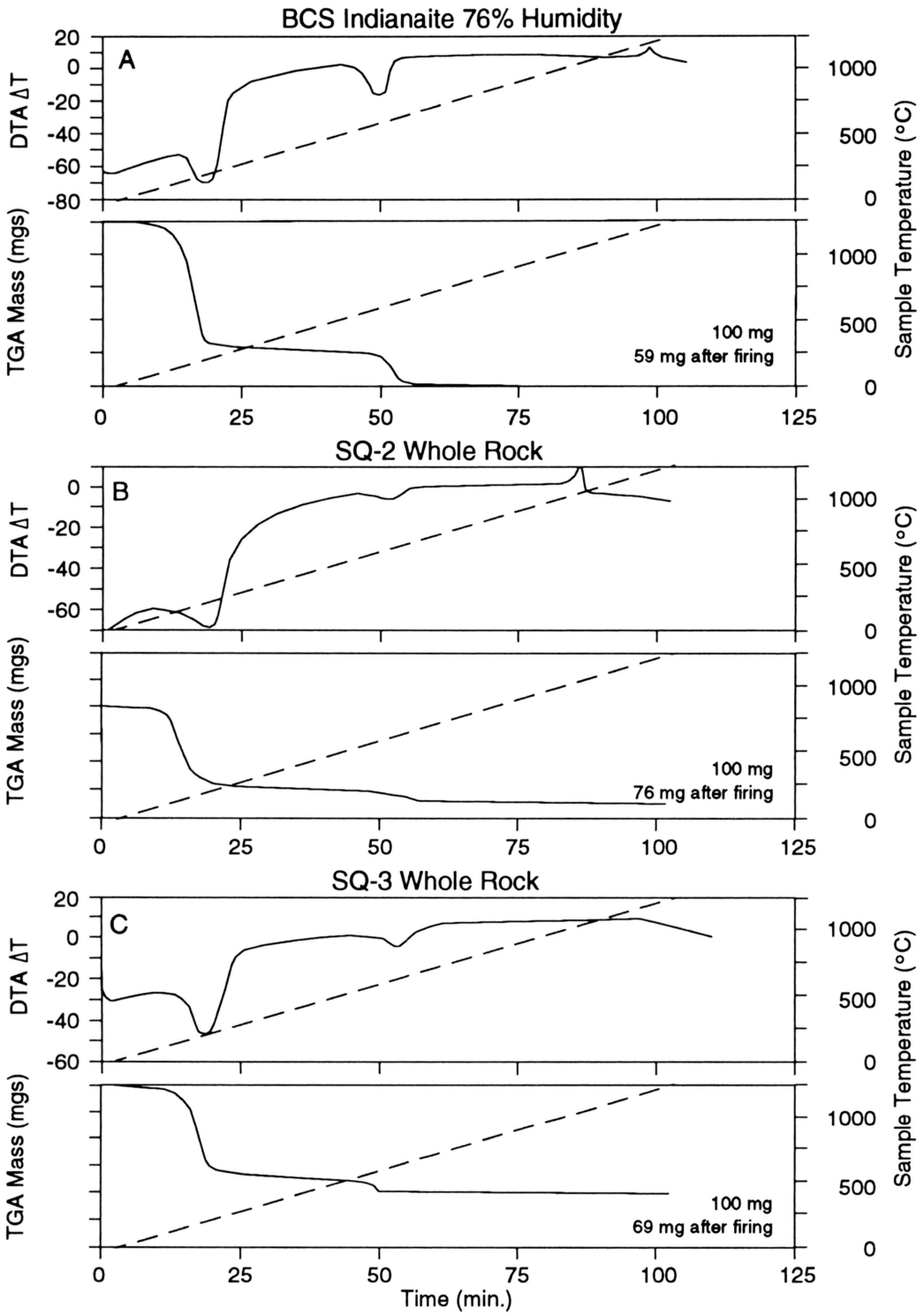

Figure 8. DTA/TGA curves for BCS indianaite (A); SQ waxy clays (B, C); GMR halloysite (10Å), (D); and GMR allophanes (E, F). Temperatures at any point along the curves are given by the dashed lines in each graph. Equal size of the 150°C and 500°C DTA endotherms and corresponding steps on the TGA curves indicate nearly pure halloysite (10Å) in a sample, such as in D. Increase in size of the 150°C endotherm and corresponding mass loss step indicate larger allophane contents of a sample. Approximately 1000°C exotherms on the DTA curves indicate mullite formation and exotherms in the region of 925°C indicate spinel formation.

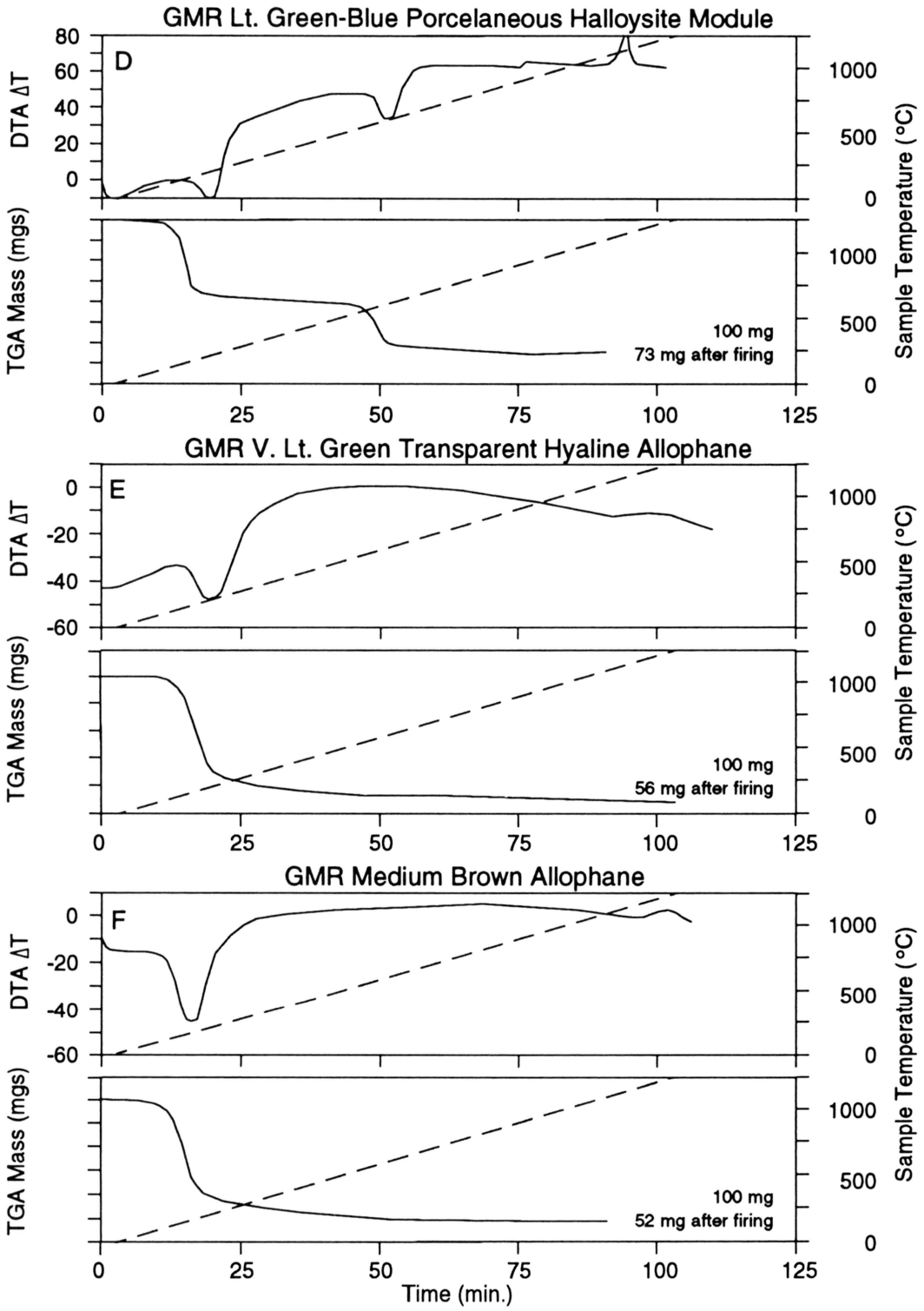

Figure 8. (cont.) DTA/TGA curves for BCS indianaite (A); SQ waxy clays (B, C); GMR halloysite (10Å), (D); and GMR allophanes (E, F). Temperatures at any point along the curves are given by the dashed lines in each graph. Equal size of the 150°C and 500°C DTA endotherms and corresponding steps on the TGA curves indicate nearly pure halloysite (10Å) in a sample, such as in D. Increase in size of the 150°C endotherm and corresponding mass loss step indicate larger allophane contents of a sample. Approximately 1000°C exotherms on the DTA curves indicate mullite formation and exotherms in the region of 925°C indicate spinel formation.

pH = 4.0) for the duration of FeS oxidation; the siliciclastic unit must extend to the weathering surface, that is, no rock units (such as limestone) can occur above which could strongly buffer the pH of descending water above the aluminum solubility break.

2) Rain water enters the siliciclastic unit through the soil zone and interacts with FeS (and other sulfides, if present) to produce sulfuric acid (reaction **1**). Meteoric water migrates through the vadose zone maintaining high oxygen content by diffusion of atmospheric oxygen into the soil and water of the unsaturated zone. Sulfide oxidation continually decreases the vadose water pH and causes dissolution of aluminous detrital minerals and apatite (reactions **2a** - **2f**).
3) Vadose water, charged with sulfuric acid and dissolved species, reaches the carbonate rock below the siliciclastic unit and reacts to neutralize the sulfuric acid (reaction **3**). Increase in pH above the aluminum solubility break causes precipitation of hydrous aluminous phases including allophane (or a lower silica precursor), hydrobasaluminite, and possibly halloysite (10Å) (reactions **4a** - **4e**). Rise in pH also causes precipitation of iron and manganese oxyhydroxides.
4) Secondary changes in the precipitates (reactions **5a** and **5b**) caused by the pH increase at the limestone interface occur as new vadose water arrives at the precipitation site, and as changes in the geometry (fracturing, displacement, compaction) of the deposit occur due to gypsum crystallization and/or dissolution of the limestone combined with overburden load. Initial precipitation occurs as soon as the aluminum solubility break (about pH = 4.0) is reached. Continued equilibration of the fluid adjacent to the limestone, however, may drive the pH of precipitates adjacent to the limestone up as high as 8.5. This pH change leads to increased silica mobility allowing reorganization of allophane to halloysite (10Å), followed by conversion of halloysite (10Å) to gibbsite. Aluminum sulfates may convert to gibbsite in this environment as well.
5) Aluminous precipitates such as those at GMR may become so thick as to prevent immediate interaction of newly arriving vadose water with the limestone substrate. In such cases, the acid is neutralized by reaction with previously formed precipitates. Diffusion of H^+ from the upper levels of an indianaite body and $(OH)^-$ from the limestone interface apparently allow neutralization to proceed even after the carbonate is coated by thick aluminous precipitates as occurs at GMR.
6) Optimal conditions for thick indianaite formation occur in situations like GMR where the vadose zone extends through a thin carbonate unit and a perched water table is formed on top of an underlying shale. Slight dip of the limestone unit combined with rapid flow of the vadose fluid to the limestone and lateral movement along the perched water table through the limestone down-dip provides excellent conditions for interaction of the acid vadose water with the surface of the limestone and the walls of caves through the limestone. Much evidence from GMR, such as blocks of sandstone incorporated in indianaite, rotated layering in the indianaite, and relic knobs of limestone with delicate dissolution shapes below the indianaite, support cavern development in the Beech Creek Limestone during earlier stages of indianaite formation.
7) Indianaite mineralization will continue as long as all of the components of the reaction path exist. Exhaustion of sulfides or aluminous detritus in the siliciclastic rock unit, complete dissolution of the limestone below the siliciclastic unit, erosion of the siliciclastic unit, and/or change in water table level to a distance above the limestone preventing interaction of the vadose water with it will cause the indianaite precipitation process to stop.

Based on this model, a few closing statements can be made about the BCS, SQ, and GMR deposits: Pyrite is rare in the weathered Bethel Formation above the indianaite at BCS, and cavernous drainage extends to nearly 30 m below the indianaite horizon. We believe that indianaite precipitation has been largely arrested at BCS because vadose water reaching the limestone is too high in pH to have interacted with aluminous detritus. As such, the water is low in $(SO_4)^{2-}$ and has high enough pH to allow gypsum and hydrobasaluminite dissolution and the formation of gibbsite and halloysite (10Å) nodules. Poor drainage from the surface of the limestone at SQ caused elevated $(SO_4)^{2-}$ concentrations and allowed the development of abundant gypsum and hydrobasaluminite. Slow fluid migration produced waxy clay, an admixture of the components arriving at the limestone surface carried by the vadose water. Indianaite precipitation was probably active when the Bethel Formation at the site was stripped. The differences of the BCS and SQ deposits show the important effect of ground-water hydrology on the type of indianaite that is produced at a given locality. Indianaite precipitation at GMR probably is arrested because of the exhaustion of FeS in the Mansfield Formation and nearly complete replacement of the Beech Creek Limestone by indianaite. Conversion of allophane to halloysite (10Å), and aluminous sulfates to gibbsite probably still continues at GMR, however.

Comparison of Results to Previous Studies

Previous studies of indianaite in Indiana and elsewhere provide explanations for the formation of this unique rock, but they do not use direct textural evidence to define the exact interactions (reactions) that produced indianaite. Although sources of sulfuric acid, aluminum, and silica are recognized in these models, no detail is given of the actual mechanisms of indianaite precipitation from fluid or neomineralization from preexisting clay.

In an early review of the genesis of indianaite, Thompson (1886) restated the idea of Cox (1875) to more clearly specify the source for silica needed for indianaite precipitation. Both workers thought aluminum and iron in indianaite were residual components from the digestion of limestone by "carbonated water." Thompson (1886) proposed that the silica in indianaite was provided by "leaching" of the overlying sandstone.

Ries (1922) suggested indianaite formed as replacement of quartz pebbles in the basal Mansfield Formation but provided only the occurrence of angular quartz grains, indianaite veins in sandstone, and blocks of sandstone in the indianaite as evidence for this model. Logan (1922b) presented a complex discussion of the formation of indianaite based on alteration of a Pennsylvanian clay body by acid waters with strong influence in the mineralization process by sulfur bacteria.

Studies prior to 1948 are summarized by Callaghan (1948) whose synthesis of new data from GMR and the older reports led to the conclusion that indianaite formed from Paleozoic weathering residuum of the Beech Creek Limestone and that only minor reorganization of this material has resulted from modern interaction with acid from iron-sulfide weathering. Note that a Paleozoic origin for indianaite is here precluded because deep burial would have converted the metastable assemblage of indianaite to kaolinite, boehmite, and apatite (Ambers, 1993).

Sunderman (1963) suggested that residual halloysitic clays developed on Chesterian limestones were reworked during Late Chesterian or Early Pennsylvanian time and deposited in Early Pennsylvanian time at the base of the Mansfield Formation. Replacement of limestone by indianaite minerals was noted by Sunderman, but he considered the effect too minor to be important in the development of the entire deposit. Keller and others (1966) proposed that the acid waters percolated into a limestone residuum which was "reconstituted" into elongate halloysite and allophane. Ettensohn and Bayan (1990) called on saturation of the acid waters and precipitation of halloysite as the water flow stagnated at a permeability barrier.

Dombrowski and others (1989) suggest that the acid waters mixed with "less acidic groundwaters from the underlying limestones" and caused a pH change that forced precipitation of "halloysite." The hypothesis of that study was that interaction of the weathering acids or "meteoric waters" was with high pH "ground-water" fluids communicating with deeper Paleozoic limestones, mostly of the Blue River Group (fig. 2). Their model does not suggest direct interaction of acidic vadose meteoric ground water with a limestone unit subadjacent to the indianaite but proposes mixing of ground waters at the water table. Several lines of evidence suggest that the model of Dombrowski and others (1989) cannot adequately explain indianaite formation:

1) Drillhole data of Callaghan (1948) show that the GMR deposit conforms closely to the position of the Beech Creek Limestone that is 35 m above the Blue River Group at GMR. Three major shale units (formations) occur between the indianaite and Blue River Group strongly limiting upward migration of ground water (fig. 2).
2) GMR and related deposits typically occur within sinuous ridges tens of meters above the level of the adjacent valley floors. This setting precludes development of a hydrodynamic head that would force cold, deep-seated ground water in the Blue River Group up through the ridges to the level of the indianaite without the water escaping laterally into the surface drainage.
3) Small springs are common along the sides of GMR at the position of the indianaite indicating a perched water table at the top of the Elwren Formation. This situation precludes any possibility of mixing between waters above the perched water table and those below.

The premise of pH change affecting the stability of dissolved species provided by Dombrowski and others (1989) appears correct, but they give no geologic evidence supporting their ground-water mixing model. Cox (1875) stated:

> the porcelain clay of Lawrence County has resulted from the decomposition, by chemical waters, of a bed of limestone and the mutual interchange of molecules in the solution, brought about by chemical precipitation and affinity.

Cox suggested an intimate genetic association of indianaite and limestone, but was not aware of the pH control on aluminum solubility or of the production of sulfuric acid by iron-sulfide weathering. The concept of water/limestone interaction directly causing indianaite formation was rejected after Thompson's statements in 1886 and has not been positively reconsidered until now.

Extension of Results to Other Halloysitic Clay Deposits

Several examples of halloysitic clays have been described that show a similar geologic setting as the indianaite deposits studied here. Well-exposed indianaite at Stanford, Kentucky has been studied in detail by Keller and others (1966), Huang and Keller (1973), and Ettensohn and Bayan (1990). The Stanford deposit is similar to the deposits in Indiana except that it occurs below weathered New Albany Shale (Devonian) which remains pyritic even after extensive weathering. The substrate of the Stanford indianaite is the Drakes Formation (Ordovician) which consists of argillaceous ankeritic dolostone. No previous study has suggested the interaction of acid meteoric water with underlaying carbonate as the mechanism for mineralization at the Stanford locality. Each study relies on the presence of weathered Brassfield Limestone residuum of Silurian age to supply components for the deposit. The occurrence is so similar to those studied here that the mechanism for the emplacement of the Indiana deposits must also apply to that deposit. A clay residuum is not necessary for the formation of indianaite and the contribution of components by such a residuum at Stanford is unlikely. Keller and others (1966) and Ettensohn and Bayan (1990) suggest this improbability but call on residuum as a component source nevertheless. A substantial portion of the minerals in the Stanford indianaite may have been derived from

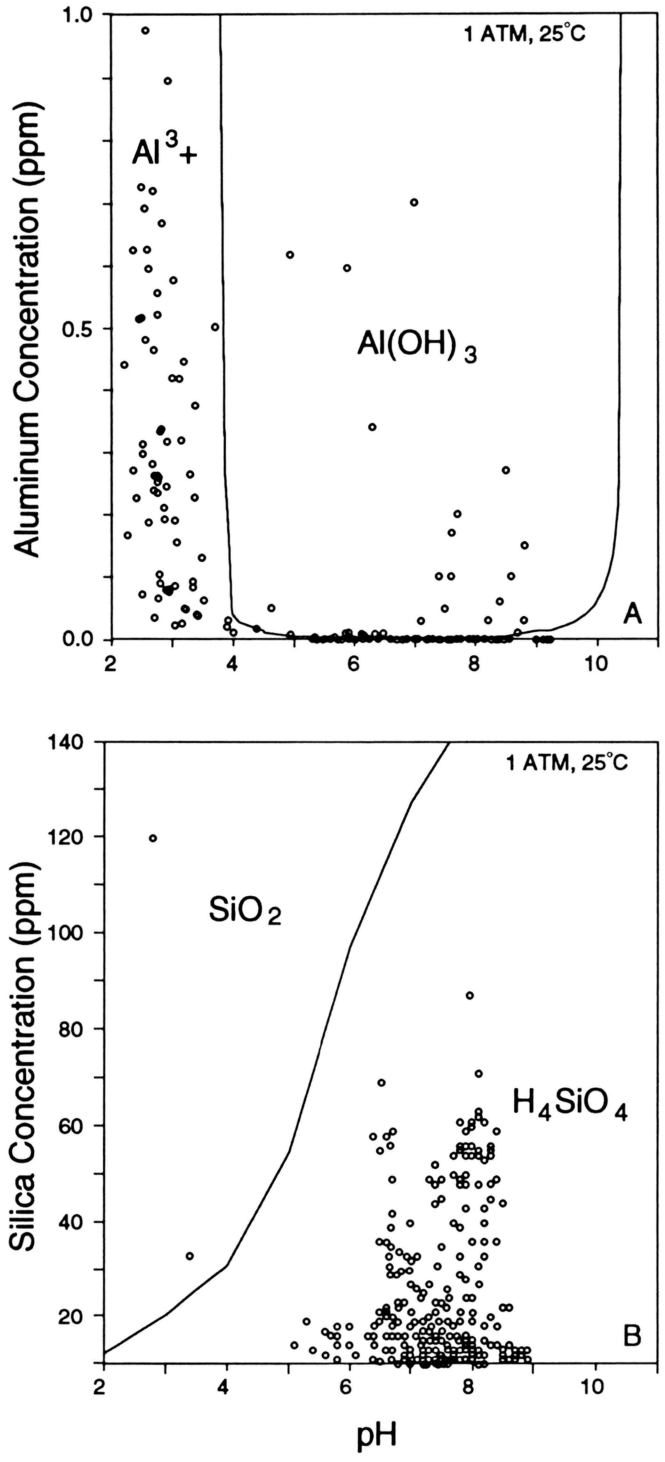

Figure 9. Solubility and pH diagrams for aluminum (A) and silica (B) modified after Mason (1952) showing the influence on aluminum and silica solubility that pH increases caused by interaction of acid sulfate water with limestone may produce. Data for natural ground waters were compiled and plotted along with the solubility curves to illustrate the typical compositions of ground waters from similar environments to those involved in indianaite formation. Stray data points in the Al_2O_3 field in (A) are waters from organic-rich sediments or rocks and show the strong influence of Al-organic complexes on aluminum solubility. Data were compiled from Meisler (1963), Back and Hanshaw (1970), Langmuir (1971), Meisler and Becker (1971), Hollowell and Koester (1975), Ruhe and others (1977), Kimball (1981), Chapelle and Drummond (1983), Royer (1983), Taylor (1984), Powell and Larson (1985), Robins (1986), Stoner and others (1987), McElroy (1988), Williams and Hammond (1988), Krause (1989), Siegel (1989), and Busby and others (1991).

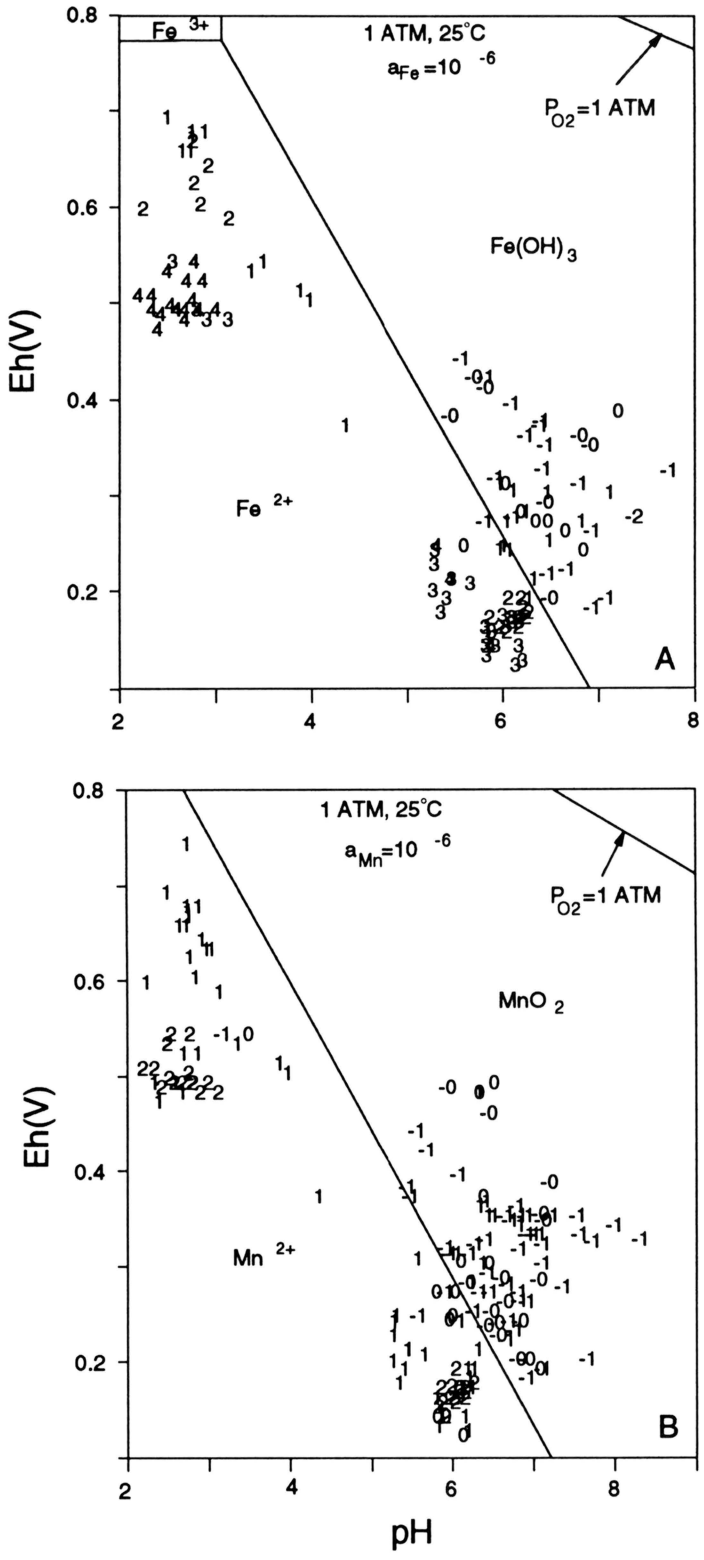

Figure 10. Eh-pH-concentration diagrams for iron (A) and manganese (B) showing data from Krause (1989) and approximate solubility boundaries in Eh-pH space for iron and manganese proposed by Ponnamperuma and others (1967) and Ponnamperuma and others (1969), respectively. Iron and manganese concentrations are shown as log ppm values rounded to the nearest whole decimal and plotted at each value's respective Eh-pH position. The data show the strong dependence of iron and manganese solubility on both Eh and pH. Note that at a constant Eh an increase in pH will cause both elements to precipitate. This is supported by the zero and negative values of the log ppm concentration numbers on the insoluble side of the theoretical Eh-pH solubility lines.

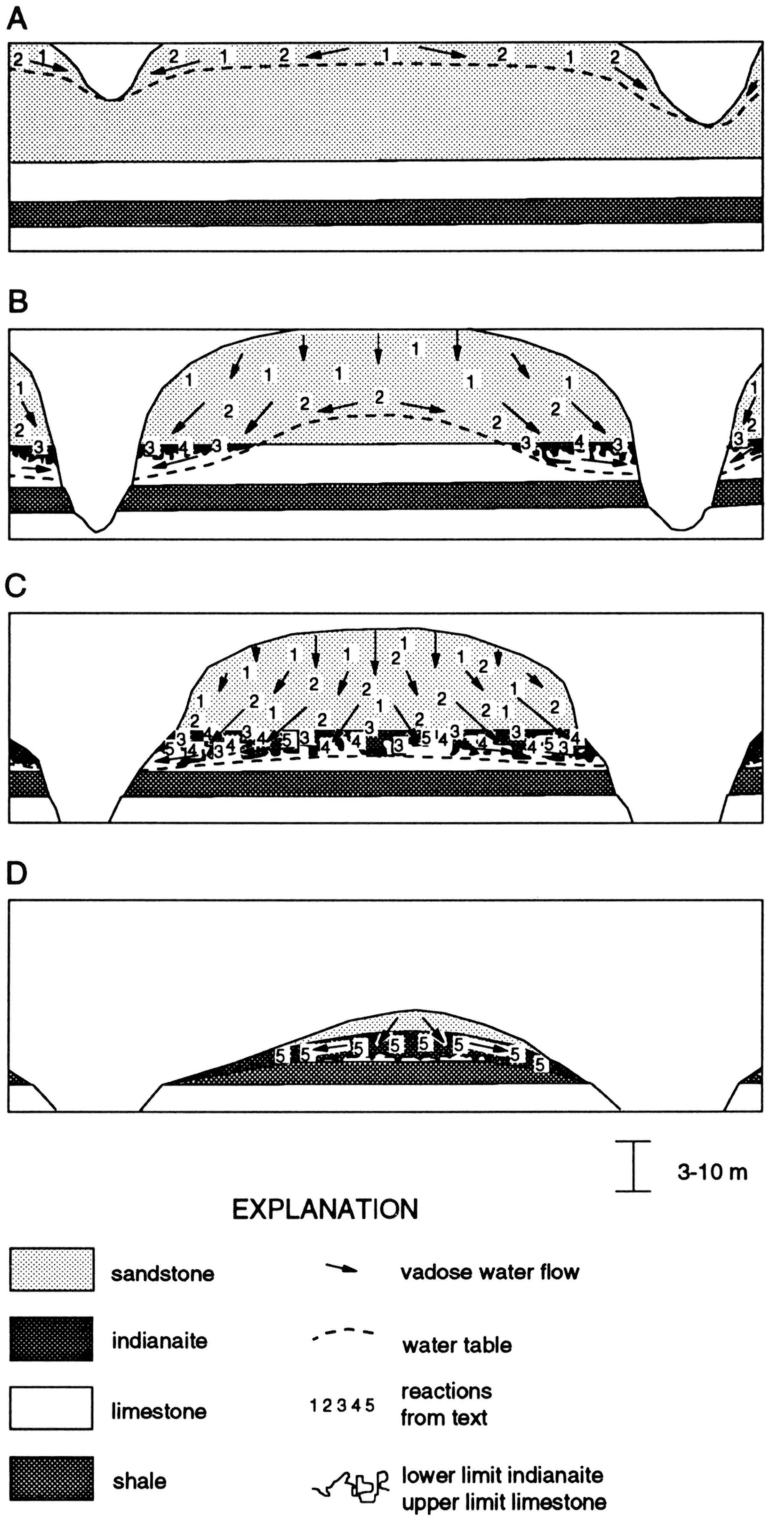

Figure 11. Model for the idealized evolution of an indianaite deposit based on the stratigraphy and rock types of the GMR deposit. A - setting during initial incision by surface drainage and weathering. B - meteoric water interaction with pyritic siliciclastic rock and vadose water migration paths set up after surface drainage incisement below the carbonate unit. C - continued development of indianaite at the upper carbonate unit contact and along internal drainages. D - the mature indianaite deposit in which ripening of early precipitates occurs as pH rises following the end of H_2SO_4 production. This sequence closely follows the inferred evolution of the GMR deposit.

the Drakes Formation, however, as sulfuric acid would remove carbonate and leave the siliciclastic residue of the dolostone behind. Lowermost indianaite horizons of the Stanford occurrence contain abundant quartz, illite, kaolinite, and chlorite (Ettensohn and Bayan, 1990), compatible with acid digestion of the dolostone. The detrital clays would be strongly affected by very low pH and may be dissolved and incorporated into allophane, halloysite (10Å), or aluminum sulfates. The Stanford locality is important in that it shows that the carbonate substrate of indianaite need not be limestone.

Hill (1990) reported that halloysitic clay nodules and coatings line and fill boxwork cavities in limestone at Carlsbad Caverns. Interaction of sulfuric acid with the limestone in Carlsbad Caverns is well documented in her study. The mechanism of aluminum- and silicon-bearing sulfuric acid waters interacting with limestone described above probably produced these deposits, although the source of acid is much different.

Halloysitic clays at the Dragon Mine located in the Tintic Mountains of Utah occur as replacement of limestone by hydrothermal fluids associated with magmatic emplacement (Kildale and Thomas, 1957). Hydrothermal fluids likely contained large amounts of sulfuric acid, which upon neutralization in the limestone precipitated the halloysitic clay.

These examples show that aluminous deposits may precipitate in situations where water acidified by sulfuric acid interacts with aluminosilicates and then is neutralized by carbonate minerals. This may explain deposits not discussed here and may be useful in exploration for areas of halloysitic clay mineralization.

Exploration For Indianaite in Indiana

The results of this study should aid future exploration efforts for high-quality indianaite clays usable for innumerable high technology ceramic, catalytic, and chemical applications. Halloysite (10Å) in porcelaneous nodules like those at GMR would be premium material for low-volume applications which require high purity. Location of economic deposits of indianaite depends on the stratigraphic succession that may allow its formation. Ideally, occurrence of FeS-bearing siliciclastic rock at the weathering surface underlain by limestone (or other carbonate rock) a short distance above the water table would provide the best opportunity for thick indianaite development. Given this situation, locating indianaite deposits should be an uncomplicated task of reviewing drill records or core and locating regions having the appropriate geology and hydrology. Target intervals in Indiana should include the outcrop belts of the base of the New Albany Shale, Bethel Formation, and Mansfield Formation. Some of the limestones overlain by black shale and/or pyritic sandstone in the middle and upper Pennsylvanian rocks of southwestern Indiana (such as in the Staunton and Dugger Formations) may also be suitable for indianaite development. Paleovalleys in the Pennsylvanian erosion surface located by Droste and Keller (1989) are especially important because they were loci of sand deposition in early Pennsylvanian time. The deposit at GMR occurs below the thick sand deposited in an upper branch of the Shoals River valley (Droste and Keller, 1989, fig. 3). Thick sandstone intervals in the West Baden Group, which occur in a clastic belt extending from Greene County southwestward (Shaver and others, 1986), have an appropriate stratigraphic sequence for indianaite formation. Study of cores and drill records already available may help delimit regions where these FeS-bearing formations overlie carbonate rock in the outcrop. Field confirmation may be useful in some localities, but drilling and test pits will be much more valuable given the poor exposure potential of indianaite.

CONCLUSIONS

This work shows that interaction of acidic vadose waters first with Al-bearing siliciclastic and then carbonate rock is the fundamental cause of indianaite formation. Interaction of acid waters with rock above the limestone is shown by degraded muscovite and etched feldspar. Oxidation of rock above the limestone is clearly indicated by limonite staining and removal of pyrite and organic matter. In cases where carbonaceous/pyritic rock overlies indianaite, as at BCS, the reduced rock is cut by oxidized joints that channelized oxygenated and acidified waters to the reaction site. Replacement textures of calcite by gypsum in the limestone underlying indianaite indicate interaction of sulfuric acid and calcite. Increase in pH due to this neutralization is the cause for precipitation of aluminous phases above the limestone. Examination of natural water chemistry suggests oxidation of FeS typically results in pH's ranging from 2.0-3.5. Aluminum contents of these waters may be as high as 1000 ppm. The paucity of published silica measurements for low pH, shallow ground waters precludes any conclusion pertaining to the behavior of silicon in these systems. Waters from carbonate buffered systems range in pH from 5.8-8.7. Aluminum concentration rarely exceeds 1 ppm and silica is as high as 100 ppm in these waters. Iron and manganese show a strong Eh-pH dependence in natural waters, whereby increasing pH generally causes iron and manganese precipitation. Rise of pH during interaction of acid water with carbonate minerals will force precipitation of aluminum, iron, and manganese dissolved from overlying rocks at low pH. Amorphous aluminum phases are precipitated as the pH rises above approximately 4.0, at which point aluminum solubility decreases abruptly. Further increase in pH as equilibrium with the limestone is approached enhances silica mobility, allowing halloysite nucleation and growth from allophane in the pH range of approximately 5.5-6.5. Gibbsite growth and replacement of aluminum silicates and sulfates stable at lower pH's occur in the pH range 6.5 to 8.7 as silica is mobilized to other parts of the system. Indianaite is a complex mixture of phases resulting from the approach to equilibrium

concomitant with evolving fluid pH. Mineral stabilities and textures are probably constrained by nucleation and growth kinetics, however this cannot be unequivocally demonstrated with the data presented here.

Field evidence suggests at least some aluminosilicate material may be derived at the site of halloysite precipitation, although a clay precursor of the indianaite is clearly not required. Thick indianaite with relict limestone below it at GMR probably results from nearly complete dissolution of the limestone by the acid sulfate water and replacement by indianaite. In essence, the indianaite-forming reaction has gone to completion in some parts of the GMR deposit because the supply of a reactant (limestone) was exhausted. Such areas of the GMR deposit will continue to equilibrate with the fluids present to produce a simple mineral assemblage dominated by halloysite, and perhaps eventually, poorly crystallized kaolinite. Erosion (or man) will probably destroy the deposit by then, however.

Carbonate rock directly affects the pH of acid water and causes precipitation of aluminous phases. Examples in this study and in several published examples show this relationship. This model predicts that halloysite and/or other hydrous aluminous phases may occur in any near-surface situation where acid waters interact first with aluminosilicate rocks and then with carbonate rocks and are neutralized. Aluminous precipitates for economic use may be located in these situations.

ACKNOWLEDGMENTS

The authors would like to thank Curtis H. Ault, Tracy D. Branam, J. Robert Dodd, John B. Droste, Rebecca K. Ambers, and Nelson R. Shaffer for critical review of the manuscript. Rebecca Ambers also helped to type additions to the text. Quarry access and transportation was provided by William O'Neal and Floyd Underhill of Rogers Group, Inc. and is gratefully acknowledged. Clay Harris, Lisbeth Kovach, Daniel Petzold, Robert Pruett and Franz Reisch provided important discussion during different stages of field work.

This research was supported by funding from the Edward J. Grassmann Trust and a student grant (#4852-92) to Clifford Ambers from the Geological Society of America. Scanning electron microscopy work was made possible by National Science Foundation grant PCM8212660.

REFERENCES CITED

Ambers, Clifford P., 1993, The nature and origin of very well crystallized kaolinite: Bloomington, Indiana, Indiana University, Ph.D. dissertation, 493 p.

Back, William, and Hanshaw, Bruce B., 1970, Comparison of chemical hydrogeology of the carbonate peninsulas of Florida and Yucatan: Journal of Hydrology, v. 10, p. 330-368.

Barnes, Ivan, and Clarke F. E., 1964, Geochemistry of ground water in mine drainage problems: United States Geological Survey Professional Paper 473-A, 6 p.

Berner, Robert A., and Holdren, George R., Jr., 1979, Mechanism of feldspar weathering-II. Observations of feldspars from soils: Geochimica Cosmochimica Acta, v. 43, p. 1173-1186.

Busby, John F., Plummer, L. Niel, Lee, Roger W., and Hanshaw, Bruce B., 1991, Geochemical evolution of water in the Madison Aquifer in parts of Montana, South Dakota, and Wyoming: United States Geological Survey Professional Paper 1273-F, 89 p.

Callaghan, E., 1948, Endellite deposits in Gardner Mine Ridge, Lawrence County, Indiana: Indiana Division of Geology Bulletin 1, 47 p.

Chapelle, Francis H., and Drummond, David D., 1983, Hydrogeology, digital simulation, and geochemistry of the Aquia and Piney Point-Nanjemoy aquifer system in southern Maryland: Maryland Geological Survey Report of Investigations, no. 38, 100 p.

Chigira, M., 1990, A mechanism of chemical weathering of mudstone in a mountainous area: Engineering Geology, v. 29, p. 119-138.

Cox, E. T., 1875, Sixth annual report of the Geological Survey of Indiana, made during the year 1874, p. 13-23.

Cox, E. T., 1879, Eighth, ninth, and tenth annual reports of the Geological Survey of Indiana, made during the years 1876-77-78, p. 154-159.

Crawford, Thomas J., and McGrain, P., 1963, Porcelaneous halloysite beneath the New Albany Shale in Lincoln County, Kentucky: Geological Society of America Special Papers 76, p. 241-242.

Diamond, S., and Bloor, James W., 1970, Globular cluster microstructure of endellite (hydrated halloysite) from Bedford, Indiana: Clays and Clay Minerals, v. 18, p. 309-312.

Dombrowski, T., Merkl, Roland S., Pruett, Robert J., Toth, T., Yuan, J., and Murray, Haydn H., 1988, A groundwater mixing model for the formation of the Indiana halloysite at the Gardner Mine, Bedford, Indiana: Clay Minerals Society 25th Annual Meeting Abstracts, p. 52.

Dougherty, Murray T., and Barsotti, Nino J., 1972, Structural damage and potentially expansive sulfide minerals: Bulletin of the Association of Engineering Geologists, v. 9, p. 105-125.

Drever, James I., 1988, The geochemistry of natural waters: Englewood Cliffs, N. J., Prentice Hall, 437 p.

Droste, John B., and Keller, Stanley J., 1989, Development of the Mississippian-Pennsylvanian unconformity in Indiana: Indiana Geological Survey Occasional Paper 55, 11 p.

Etherington, John R., 1975, Environment and plant ecology: London, John Wiley and Sons, 347 p.

Ettensohn, F. R., and Bayan, M. R., 1990, Occurrence and significance of a zoned halloysite, (10Å) and allophane deposit below Devonian black shales in central Kentucky: Southeastern Geology, v. 31, p. 1-25.

Gray, H. H., 1990, Map of Indiana showing the bedrock geology: Indiana Geological Survey Miscellaneous Map No. 48.

Greenberg, Seymour S., and Sunderman, A., 1961, Association of porcelaneous halloysite with a friable lower Pennsylvanian quartz conglomerate in Indiana: Geological Society of America Special Papers 68, p. 185.

Hem, J. D., 1959, Study and interpretation of the chemical characteristics of natural water: United States Government Printing Office, Washington, D.C., 269 p.

Hill, Carol A., 1990, Sulfuric acid speleogenesis of Carlsbad Cavern and its relationship to hydrocarbons, Delaware Basin, New Mexico and Texas: American Association of Petroleum Geologists Bulletin, v. 74, p. 1685-1694.

Hollowell, Jerrald R., and Koester, Harry E., 1975, Ground-water resources of Lackawanna County, Pennsylvania: Pennsylvania Geological Survey Water Resource Report, v. 41, 106 p.

Huang, W. H., and Keller, W. D., 1973, New stability diagrams of some phyllosilicates in the SiO_2-Al_2O_3-K_2O-H_2O system: Clays and Clay Minerals, v. 21, p. 331-336.

Keller, W. D., McGrain, P., Reesman, A. L., and Saum, N. M., 1966, Observations on the origin of endellite in Kentucky, and their extension to "indianaite," *in* Proceedings from the 13th National Conference on Clays and Clay Minerals, p. 107-120.

Kildale, M. B., and Thomas, R. C., 1957, Geology of the halloysite deposit at the Dragon Mine, *in* Guidebook to the geology of Utah, no. 12: Salt Lake City, Utah, Utah Geological Society, p. 94-96.

Kimball, Briant A., 1981, Geochemistry of spring water, southeastern Uinta Basin, Utah and Colorado: United States Geological Survey Water-Supply Paper 2074, 30 p.

Kissling, D. L., 1967, Environmental history of lower Chesterian rocks in southwestern Indiana: Bloomington, Indiana, Indiana University, Ph.D. dissertation, 367 p.

Krause, Linda J., 1989, Analysis of groundwater chemistry at a reclaimed coal mining site, Wheatland, Indiana: Bloomington, Indiana, Indiana University, M.S. thesis, 118 p.

Langmuir, D., 1971, The geochemistry of some carbonate ground waters in central Pennsylvania: Geochimica Cosmochimica Acta, v. 35, p. 1023-1045.

Logan, W. N., 1922a, Indianaite of Indiana: general features of the deposits, *in* High grade clays of the eastern United States: United States Geological Survey Bulletin 708, p. 147-154.

Logan, W. N., 1922b, Economic geology of Indiana, *in* Handbook of Indiana geology: Indiana Department of Conservation Publication 21, pt. 5, p. 571-1058.

Mackenzie, R. C., 1970, Differential thermal analysis: London and New York, Academic Press, 775 p.

Mason, B., 1952, Principles of geochemistry: New York, John Wiley and Sons, 274 p.

McElroy, Thomas A., 1988, Groundwater resources of Fayette County, Pennsylvania: Pennsylvania Geological Survey Water Resource Report 60, 57 p.

Meisler, H., 1963, Hydrogeology of the carbonate rocks of the Lebanon Valley, Pennsylvania: Pennsylvania Geological Survey Bulletin W18, 80 p.

Meisler, Harold, and Becher, Albert E., 1971, Hydrogeology of the carbonate rocks of the Lancaster 15-Minute Quadrangle, southeastern Pennsylvania: Pennsylvania Geological Survey Bulletin W26, 149 p.

Merino, E., Harvey, Colin, and Murray, H. H., 1989, Aqueous-chemical control of the tetrahedral-aluminum content of quartz, halloysite, and other low-temperature silicates: Clays and Clay Minerals, v. 37, p. 135-142.

Ponnamperuma, F. N., Loy, T. A., and Tianco, F. M., 1969, Redox equilibria in flooded soils, II. The manganese oxide systems: Soil Science, v. 108, p. 48-57.

Ponnamperuma, F. N., Tianco, E. M., and Loy, T. A., 1967, Redox equilibria in flooded soils, I. The iron hydroxide systems: Soil Science, v. 103, p. 374-382.

Powell, John D. and Larson, Jerry D., 1985, Relation between groundwater quality and mineralogy in the coal-producing Norton Formation of Buchanan County, Virginia: United States Geological Survey Water-Supply Paper 2274, 30 p.

Quigley, R. M., and Vogan, R. W., 1970, Black shale heaving at Ottawa, Canada: Canadian Geotechnical Journal, v. 7, p. 106-115.

Ries, H., 1922, Indianaite of Indiana—the deposit of indianaite near Huron, Lawrence County, Indiana, *in* High grade clays of the eastern United States: United States Geological Survey Bulletin 708, p. 154-162.

Robins, N. S., 1986, Groundwater chemistry of the main aquifers in Scotland: British Geological Survey BGS Report 18, no. 2, 57 p.

Rock Color Chart Committee, 1984, Rock color chart: Geological Society of America, 6 pl., 2 p.

Ross, Clarence S., and Kerr, Paul F., 1935, Halloysite and allophane: United States Geological Survey Professional Paper 185-G, 148 p.

Royer, Denise W., 1983, Summary groundwater resources of Lebanon County, Pennsylvania: Pennsylvania Geological Survey Water Resource Report 55, 84 p.

Ruhe, Robert V., Duigon, Mark T., and Risser, Dennis W., 1977, Environmental baseline study of ground and surface waters, Wilson Field Site, Knox County, Indiana: Bloomington, Indiana, Indiana University, Water Resources Research Center, 101 p.

Shaffer, Nelson R., 1978, Indianaite, the rock with a past: Outdoor Indiana, v. 43, p. 35-38.

Shaver, Robert H., Ault, Curtis H., Burger, Ann M., Carr, Donald D., Droste, John B., Eggert, Donald L., Gray, Henry H., Harper, Denver, Hasenmueller, Nancy R., Hasenmueller, Walter A., Horowitz, Alan S., Hutchison, Harold C., Keith, Brian D., Keller, Stanley J., Patton, John B., Rexroad, Carl B., Wier, Charles E., 1986, Compendium of Paleozoic rock-unit stratigraphy in Indiana-a revision: Indiana Geological Survey Bulletin 59, 203 p.

Siegel, D. I., 1989, Geochemistry of the Cambrian-Ordovician aquifer system in the northern Midwest, United States: United States Geological Survey Professional Paper 1405-D, 76 p.

Steefel, Carl I., and van Cappellen, P., 1990, A new kinetic approach to modeling water-rock interaction: the role of nucleation, precursors, and Ostwald ripening: Geochimica Cosmochimica Acta, v. 54, p. 2657-2677.

Stolzy, Lewis H., 1974, Soil atmosphere, *in* The plant root and its environment, E. W. Carson, ed.: Charlottesville, University Press of Virginia, p. 335-361.

Stoner, Jeffrey D., Williams, Donald R., Buckwalter, Theodore F., Felbinger, John K., Pattison, Kenn L., 1987, Water resources and the effects of coal mining, Greene County, Pennsylvania: Pennsylvania Geological Survey Water Resource Report 63, 166 p.

Stumm, Werner, and Morgan, James J., 1981, Aquatic chemistry—an introduction emphasizing chemical equilibria in natural waters: New York, John Wiley and Sons, 780 p.

Sunderman, Jack A., 1963, Mineral deposits at the Mississippian-Pennsylvanian unconformity in southwestern Indiana: Bloomington, Indiana, Indiana University, Ph.D. dissertation, 115 p.

Taylor, Larry E., 1984, Groundwater resources of the Upper Susquehanna River basin, Pennsylvania: Pennsylvania Geological Survey Water Resource Report, v. 58, 136 p.

Thompson, M., 1886, The clays of Indiana, *in* Indiana Department of Geology and Natural History Annual Report 15: Indianapolis, Indiana, p. 34-40.

Williams, Robert S., Jr., and Hammond, Stephen E., 1988, Soil-water hydrology and geochemistry of a coal spoil at a reclaimed surface mine in Routt County, Colorado: United States Geological Survey Water-Resources Investigations Report 86-4350, 100 p.

Wollast, R., 1967, Kinetics of the alteration of K-feldspar in buffered solutions at low temperature: Geochimica Cosmochimica Acta, v. 31, p. 635-648.


UNIVERSITATIS SIGILLUM
INDIANENSIS
MDCCCXX


INDIANA GEOLOGICAL SURVEY 1837
INDIANA UNIVERSITY